Questo documento, la presentazione, tutti i risultati ed il lavoro che hanno richiesto è fatto in memoria di Nonna Elisa. Mi manchi, e spero che tu possa vedermi quando mi daranno il cappello da dottore.

A One-Dimensional Model for Neuronal Growth

Stefano Perna
Centre for Mathematical Sciences - LTH
Dipartimento di Matematica "Federigo Enriquez"
Università degli Studi di Milano

8th March 2013

The notion that "applied" knowledge is somehow less worthy than "pure" knowledge, was natural to a society in which all useful work was performed by slaves and serfs, and in which industry was controlled by the models set by custom rather than by intelligence.

JOHN DEWEY
Democracy and Education

Abstract

A mathematical model for neuronal growth is presented, describing the process of axonal elongation. The main construction material is a protein called tubulin, which is produced in the *soma* (core body of the cell), and transported inside the axon to a structure known as *the growth cone* on its tip, where the construction process occurs. The concentration of tubulin is modelled by a convection-diffusion PDE along the axon and by an ODE in the small tip. The length of the axon as a function of time is given by another ODE which models the building process in the growth cone. The entire model constitutes a coupled moving-boundary problem for which a numerical method is described and investigated. Simulation are also presented with parameter values from literature in the case of the squid (*Loligo pealeii*).

Contents

Introduction

All the different parts of the animal body are intended to work together for a common goal (survival, perhaps even sentient life). The director of these coordinated effort is the nervous system, which structure may differ greatly from species to species. In mammals such as our species, the nervous system is composed of a a network of sensors and processors known as neurons, part of which is located in a central "processing core" (the brain). The rest is distributed throughout the body, connected to each other through long electrical cables called axons. These connectors allow for the brain to send and receive signals to and from every part of the body, allowing it to regulate and command whatever is necessary for the task at hand.

Distruption of this inner network can bring impediments to the normal execution of everyday life, from minor (temporary loss of motor and sensory functions due to blockage of nerve conduction, called *neurapraxia*) to major life-threatening ones (paralysis of muscles connected to the neuron and loss of all sensory function due to severing of the axon - *axonotmesis* - or the neuron itself - *neurotmesis*). In extreme cases, such as critical injuries to the spinal nerve, this can compromise the survival of the organism itself.

Moreover, specific axon-damaging diseases that do not require external interactions (such as impacts or slashes) have been discovered and classified for example the *Guillan Barre Syndrome* and *Friedreich's ataxia*; it is also known that axonal damage can be a by-product of metabolic diseases like diabetes and renal failure. Assumption of chemical substances (alcohol, drugs, even chemotherapy) or specific poisons (neurotoxins) can also result in axonal damage and degeneration.

Investigating and understanding how axons grow and regenerate is the key to provide new, useful treatments for this ailments. The study of peripheral nerve injury and regeneration began during the American Civil War and has since expanded to determining therapies that enhance nerve regeneration such as biological conduits and administration of growth promoting molecules [Wikc]. However, a full understanding of the inner mechanisms of neuroregeneration, such as critical factors that promote or hinder axonal growth and how to optimize these effects is still far away [Wikd].

In this work, a mathematical model for describing axonal growth is presented. The model is an augmented version derived from the work of D. McLean and B. Graham [DRM04] and consists of a coupled set of one partial differential equation (PDE) and two ordinary differential equations (ODEs) with boundary and initial conditions. The PDE models the variations of the concentration of two globular proteins, α-tubulin and β-tubulin (collectively referred as *tubulin*). These proteins are the main building material for *microtubules*, tubular polymers which compose the "skeleton" of the axon itself. These microtubules are assembled at the tip of the growing axon, in a structure known as the *growth cone*. Tubulin flows from the center of the neuronal cell to this growth cone, where it is assembled at a rate proportional to the amount of tubulin available and modelled by an ODE. The final ODE models the variation of said concentration of tubulin in the growth cone itself.

The problem takes the form of a *Stefan's task*[1] for which an analytical solutions cannot be computed by hand. A Steady-State approach has also been undertaken, which lead to proving the absence of any such solutions. Successively, an algorithm was developed to approximate the solutions numerically using the programming software *Matlab*$^{\text{TM}}$. This follows a semi-implicit Euler approach in time and a finite difference scheme for approximating spatial derivatives. In order to accomodate the moving-boundary nature of the problem, a time-increasing mesh of the spatial domain was implemented which takes into account the effect of axonal growth.

[1] **Jožep Stefan** (24 March 1835 7 January 1893) was a Slovene physicist, mathematician, and poet who first attempted to solve this general class of moving-boundary problems around 1890, in relation to problems of ice formation. He is best known for his contributions to the formulations of the *Stefan-Boltzmann Law* for the radiation of a black body and his study in electromagnetic equations.

The model has been implemented using parameters from the Longfin inshore Squid (*Loligo Pealeii*) in order to investigate the dependence of axonal growth from different factors, such as the starting length of the growing axon or the amount of tubulin injected in the axon's body from the soma. Preliminary results indicate that critical factors that enhance axonal growth are the length of the growth cone and the speed of microtubule assembly in the growth cone itself. The tubulin income from the soma seems also to have an effect on the speed of the growth: specifically, after the first few hours of axonal growth, a drop in the subsequent flux of the chemical does not affect the process in significant ways; on the other hand, lower level of tubulin in the first hours of grow will result in a slower growth rate.

Chapter 1

Neurons, Axons, Nervous System

> If the mind is empty, it is always ready for anything; it is open to everything. In the beginner's mind there are many possibilities, in the expert's mind there are few.
>
> SHUNRYU SUZUKI
> *Zen Mind, Beginner's Mind*

In the first chapter of the work, a brief introduction to the structure of the human nervous systems will be given, in order to introduce the reader to the basic concepts of neurons, axons and axonogenesis.

The chapter is organized as follows: Section 1.1 deals with the whole Nervous Systems in the human body. In Section 1.2, the structure of neurons, how they connect to each other and how signals move between different neurons will be discussed (briefly). Fundamentals of Axonogenesis (i.e. the formation of axons from neuronal cells during prebirth) are introduced in Section 1.3, as well as some insight of its importance (both for the normal functioning of the human body *ensemble* and in relation to neurodiseases). Finally, Section 1.4 of the chapter will introduce models already in use by scientists to investigate neuronal growth and axon guidance problems.

1.1 The Human Nervous System Generalities

Like most animal species, the human body can be roughly seen as a set of *organ systems* which are linked together in various ways and each contribute to the survival and fitness of the full being. Examples of these systems are the *Circulatory System*, the *Digestive System*, *etc.* One particular organ system present in almost every[1] animal species is the *Nervous System*.

The nervous system is responsible for the coordination and syncronized functioning of an animal being, as well as providing internal control of the well-state of the organism and dealing with stimuli from the surrounding world. The human nervous system can be divided into two parts (see Figure 1.1):

1. the *Central Nervous System*;
2. the *Peripheral Nervous System*.

The *Central Nervous System* is where most of the information is processed, analyzed and stored. The main organ is the *brain*, but the *spinal cord* plays also an important role.

[1] But not all. Sponges, for instance, have no real "nervous system", even tough they are able to respond to the surrounding environment.

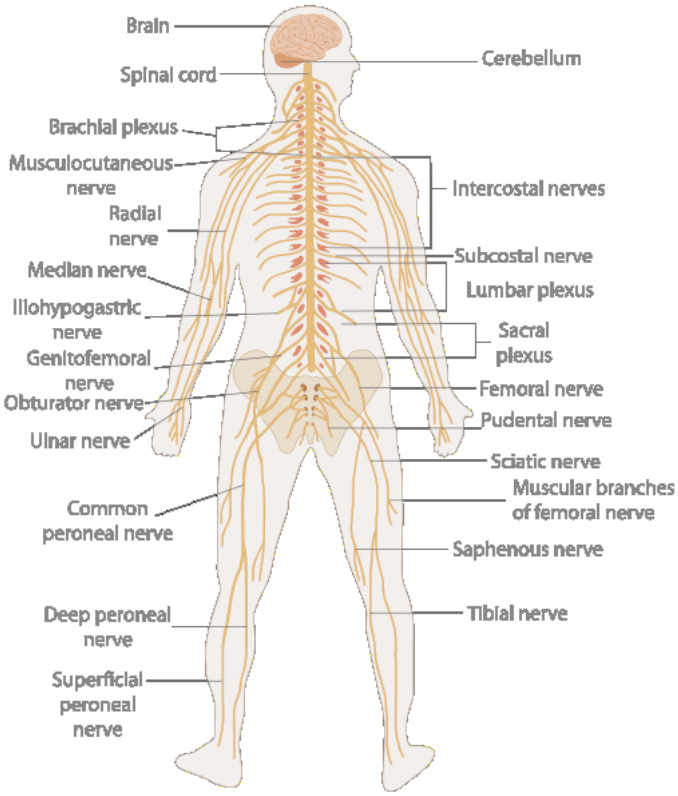

Figure 1.1: Stylized illustration of the human nervous system, showing central parts and most important nerves. Image courtesy of *Wikipedia* (*en.wikipedia.org/wiki/Nervous_System*).

The *Peripheral Nervous System* deals with the reception of signals from both different parts of the organism and the external environment, and transportation of said signals through the body, up to the Central Systems. Its main components are *neurons* and *nerves*. In the following, the main topic of analysis will be almost exclusively the Peripheral Nervous Systems (therefore called the "peripheral system"). For any reader interested in knowing more about the Nervous System in itself, we can advise any good human anatomy manual.

1.2 Neurons, Axons and Nerves

The most basic unit that forms up the peripheral system is the *neuron cell* (or simply *neuron*) (Figure 1.2. Neurons are connected to each other by *axons*. A long bundle of axons that stretches from one point of the body to another is called a *nerve* (or sometimes a *nerve cell*).

1.2.1 Neurons

The neuron can be described as *"an electrically excitable cell that processes and transmits information by electrical and chemical signaling."* [Wikb]. A neuron is a complex cell, which we can split into two parts:

- a core body called the *soma*, which contains the *nucleus* of the cell and most of the *organelles*[2];

[2] *Organelles* are subcellular structures responsible for the good functioning of the cell itself. Any more details regarding them go beyond the purpose of this chapter: for more details, consult the same good human anatomy manual.

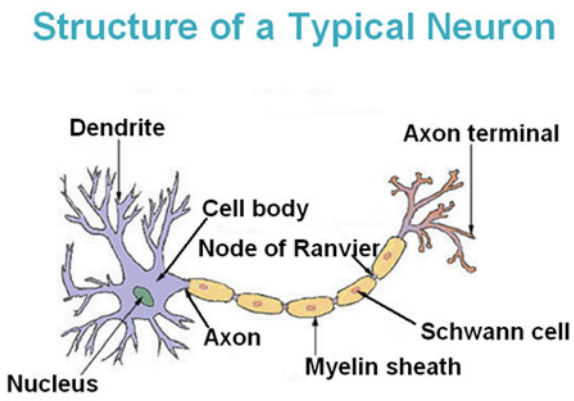

Figure 1.2: Structure of a typical neuron. Image courtesy of *Wikipedia* (*en.wikipedia.org/wiki/Neuron*).

- elongations that extrude from the soma, collectively knows as the *neurites*;

Neurites can more specifically be separated into two subtypes: *dendrites* and *axons*. Axons' morphology and function will be discussed in the following section. As for *dendrites*, they are branched "projections" of the soma, which function is to forward the electrical stimuli coming from others neurons or cells to the central *soma*.

1.2.2 Axons

As mentioned before, one particular type of neurite is the axon. An *axon* is *"a long, slender projection of a nerve cell, or neuron, that typically conducts electrical impulses away from the neuron's cell body"* [Wika]. As a general rule, neurons possess no more than one single axon[3], while some may have none. Some axons present branches, at times a lot of them, along their length. Axons form up bundles throughout the body length, called *nerves*. The length of this nerves varies greatly, from 1 millimeter or less (inhibitory interneurons) to more the one meter (the *sciatic nerve*, running from the base of the spine to the two big toes). Axons are enveloped in a dieletric substance called *myelin*, which promotes fast transmission of electric signal via a mechanics known as *saltation* of the action potential. Myelin is made up by cells known as *glial cells*, which protect and support the axon itself and its activity as a signal transmitter. Axons contact other cells (usually neurons) at *synapses*, where its membrane closes up with the target, and special molecular structures transmit signals.

1.2.3 Signal Transmission and Action Potential

So far we know that axons are responsible for transmission of signals throught the human body, from neuron to neuron. But how does this exactly work? one could ask. Modelling of this mechanisms has received a lot of interest and effort from scientists of all related disciplines.

However, the first detailed model came from Hodgkin & Huxley [ALH52a] after a series of studies on the giant axons of the squid (*Loligo Pealeii*).

The soma (central part of the neuron) is connected to its axon through the so-called *Axon hillcock*. The hillcock's voltage is directly connected to the action potential phenomenon. Dendrites connect the soma to other neurons or to an axon from another cell via synapses. Whenever a signal arrives from said other cell, it begins to change (increase or decrease) the electric potential in the *presynaptic* neuron (the neuron which is sending the signal). This variation may

[3]This should not be considered a straight claim, since the author could not find any reliable source to cite for this assessment.

induce the opening of a channel for ions inside the sypnapse (typically sodium or calcium ions) which forwards the variation of potential to the entire *postsynaptic* neuron, including its axon hillcock (as modelled by the *cable equation*). Should the potential in the hillcocks rise above a certain threshold, called *action potential threshold*, another signal will be sent towards the axon from the hillcock, which will be the new action potential. The action potential may be generated by the soma itself, or be a consequence of external stimuli. For instance, in sensory cells, the aforementioned opening of ion channels is generated by external signals, such as heat, light or a pitched sound. It is interesting to note that the amplitude of the action potential itself is not dependent on the strenght of the signal which generates it. Either it occurs completely, or it does not occur at all.

As a final note, recall that axons are wrapped up in myelin. Not only does myelin promote the transmission, but being a dieletric material, it prevents ions from escaping or entering the axon, therefore inhibiting information loss or signal degradation throughout the transmission. The mean conduction velocity of an action potential in a myelin-sheated axon ranges from 1 m/s to 100 m/s, depending on the signal and axon's diameter.

1.3 Axonogenesis

It is now interesting to discuss the formation and development of axons, as this will be a major topic in the following chapters. The process with which neurons direct their axons to one (or more) target cells is known as *axon guidance* (sometimes *axon pathfinding*). Whenever one takes into account also the rate and growth of the axon itself, the whole subject takes the name of *axonogenesis*[4].

During prebirth, neurons are generated from the *ectoderm*, the outermost cellular layer of the embryo. When the soma is fully formed, the neuron begins to sprout small projections known as *neurites*. After an initial stage and throught a process not fully understood yet, one of these neurites exihibits a dramatic increase in growth, becoming thus the *axon*. The axon then starts to extend and elongate seeking its target in the body. This stage is mainly guided by the highly mobile and sensitive tip of the newborn axon, knows as the *growth cone* (Figure 1.3). The existance of such growth cone was first postulated by Santiago Ramón y Cajal[5] in 1890,

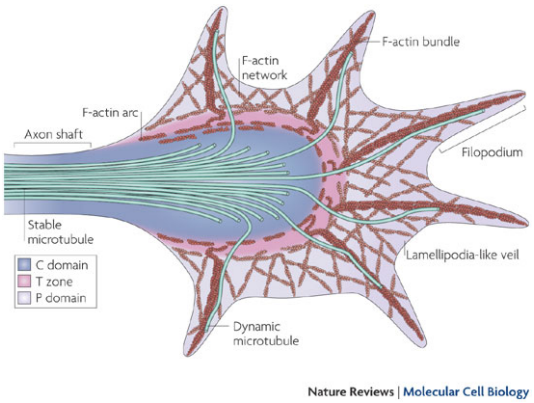

Figure 1.3: Illustration of a growth cone, showing the most important parts (not all are described in the paper). Image found on *http://www.nature.com/nrm/journal/v10/n5/box/nrm2679_BX1.html*.

[4]From the Greek word $\gamma\varepsilon\nu\varepsilon\sigma\iota\varsigma$, meaning "origin".

[5]**Santiago Ramón y Cajal** (1852-1934) was a Spanish pathologist, histologist and neuroscientist. He is considered by many to be the father of modern neuroscience. In 1906 he was awarded the Nobel Prize in Physiology or Medicine together with Camillo Golgi.

who described it as a *"a concentration of protoplasm of conical form, endowed with amoeboid movements"* [Caj90]. The growth cone can be roughly described as a central trunk from which several small tube-like branches (called *filopodia*) depart. Filopodia are highly receptive of certain substances in the surrounding environment and act like sensors which guide the axon towards its intended target via indications given by such chemical reactions. The growth cone is very dynamic and reactive, and can engage in rapid movement in response to various stimuli. The tip of the cone is constantly being augmented, thus giving birth to the elongation process.

Growth cones, as mentioned, are highly responsive to chemical substance in the body environment. Such *chemical cues* can attract or repel the growth cone, depending on the context. Both fixed and diffusible cues have been observed [NSS07]; the reaction to these cues by the growth cone is to affect its internal proteic structure, or *cytoskeleton*: if a gradient of guidance cue is found, cytoskeletal changes happen asymmetrically and the growth cone turns toward or away from the guidance cue. Biologists have identified several kinds of these chemical cueing substances [MB07].

Axonogenesis is, as one can easily speculate, a foundamental process of the human development. Failure in this process can cause several cognitive, sensorial and motor disfunctions. Also, nerves and axons can become damaged as a consequence of wounds and traumas: spontaneus axonogenesis and nerve tissue engineering are the only known way to repair damage in such vital part of the body.

1.4 Mathematical Modelling of Neurons, Axons & Axonogenesis

In this final section the reader will be introduced to some of the results and models already known in literature that deal with the topics discussed so far. Details of each equation will not be given because doing so would divert from the purpose of this chapter. Throughout the whole section, extensive use of the paper [BPG06] by Bruce P. Graham and Arjen van Ooyen will be made.

As written in this paper, most recents models (up to the last decade) deal with one specific aspect of the neurite outgrowth: Graham and van Ooyen have proposed the following four major topics of research:

1. **Neurite initiation and differentiation.** The first problem concerns the initial formation of neurites and how one of them becomes the axon, while the others remain dendrites. This problem was investigated by Hentschel and collegues in papers from 1994-98 (see for instance [HGEH96]). They assumed that initial neurite outgrowth is triggered by reaction to small inhomogeneities on the newborn cell's surface. Calcium is considered to be responsible for this trigger. It is also assumed that further elongation of the neurites is limited by the presence of a certain chemical (let it be c) which nature is not described. The situation can be summarized in a set of coupled ordinary differential equations for the variables c_0 (concentration of chemical in the soma), c_i, $\forall i = 1, \ldots, n$ (concentration in n neurite spots) and l_i (length of the neurite number n). The fourth equation,

$$\frac{dl_i}{dt} = \alpha c_i \ (\alpha > 0),$$

   is particularly interesting, as it states that the rate of elongation of the neurites is directly proportional to the concentration of said unknown chemical. Should there be a neurite with slightly longer initial length than the others, a dynamic can be observed such that said neurite will show a very rapid initial growth while the others will exihibit only very slow growth (if any at all), thus modelling the growth of the axon itself.

2. **Neurite elongation.** Work has been done to model the process of elongation of the neurite after initiation, in particular via modelling of the cytoskeleton dynamics. The fundamental variable here is the amount of available free tubulin at the tip of the neurite, and growth is limited by tubulin production rate and transportation to the site. One of the most advanced models has been developed by McLean and colleagues (see for instance [DRM04]) and consists in a set of ordinary and partial differential equations in space (1-dimensional) and time for the concentration of free tubulin and length of the neurite.

3. **Axon Pathfinding.** As mentioned, one critical ability of a newborn axon is its ability to find the way to its synaptic target. Modelling has been targeted at understanding the growth cone's sensibility to chemical cues, its steering ability and bundling of several axons into nerve tracts. Graham and van Ooyen cite the work of Aeschlimann[Aes00] in which the growth of the axon is studied in a simplified case (no branching, two-dimensional space environment). The models contains both a deterministic component (in the form of coupled ODEs for neurite elongation, as mentioned) and a probabilistic one (for the description of filopodia formation). There is also another simplified model from Maskey *et al.*[SM04] in which the change in direction is modelled by either a stochastic process or repulsion from chemical cues mechanics. Implementation of this makes use of sink - source mechanics, which then yields an equation for the change of position of each growth cone which in turn depends on the gradient of attractive or repulsive cues.

4. **Neurite Elongation and Dendritic Shape Formation.** Models for branching of neurites have been developed, both for branching of the growth cone or split-formation of a branch from the main body of a neurite. Models can be divided in one type that consider cystoskeletal dynamics and another that deals with external influences on the cone. More sophisticated models can keep into account both factors or others, like statistical factors or different chemical substances.

Chapter 2

Modelling Axonal Growth

> We have no idea about the 'real' nature of things ... The function of modeling is to arrive at descriptions which are *useful*.
>
> RICHARD ANDLER & JOHN GRINDER
> *Frogs into Princes: Neuro Linguistic Programming*

In this chapter, the model developed in order to study the axonal growth probelm will be presented. The chapter is structured as follows:

- A brief introduction to the setting of the problem will be given in Section 2.1;
- Sections 2.2 – 2.4 deal with the actual modelling, ranging from assumptions that have been made to the equations written, both for the interior of the axon and the growth cone, as well as the boundary conditions;
- Section 2.5 presents the model itself in its final form.

2.1 Setting

In the studies of human axons and axonal growth, much of the knowledge now available has been acquired by the study of animals. In particular, the squid (specifically the species *Loligo pealei*) is often used as a model test subject for various experiments in this field. Squids are

Figure 2.1: A Longfin Inshore Squid, species *Loligo pealei*.

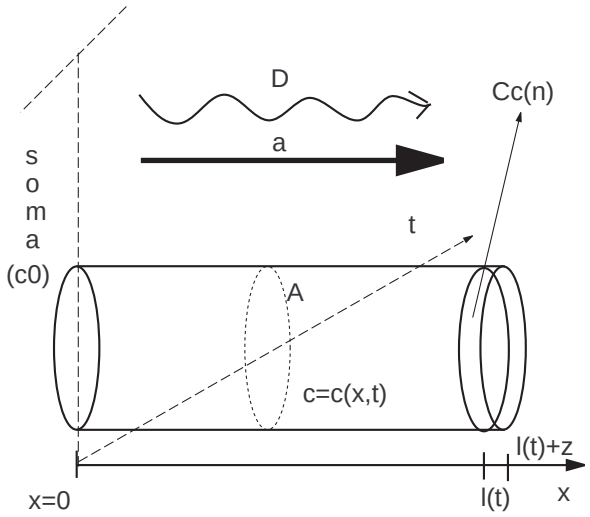

Figure 2.2: Schematic illustration of a Growing Axon.

cephalopods, purely marine animals who exihibit a bilateral body symmetry, typical prominent head (see Figure 2.1) and a set of tentacles. Squid are on average 60 centimeters long, although some species (for instance the *Colossal Squid*) can reach up to 13 meters [Wike], and exhibit relatively high intelligence among invertebrates.

Squid are often object of study due to the peculiar morphology of this creature, who exihibit a very thick axon running along the body (the so-called *giant squid axon*). In the second half of the 1900s Hodgkin and Huxley [ALH52b] conducted some pioneering work in neurochemistry and biochemistry of the brains by presenting a model for action potential in the giant squid axon. This axon is thick enough to allow for one to conduct research even with limited technology and equipment, such as the ones these two gentlemen had available.

It is interesting to point out that the nature of axons in the squid is similar to the one in human being, so with little adjustment in parameters this model could be used to simulate and investigate axonal growth in our species as well.

2.2 The Model

In this section, the model for the growth of the giant squid axon shall be presented. Some idealizing assumptions will be made to simplify calculations, as is often the case during modelling work.

2.2.1 Modelling Assumptions

The model shall be presented as a PDE / ODE model in two independent variables: time (t) and space (x, one dimension). One way to visualize this is to consider *arc coordinates* along the axon's length. All quantities will be given in SI units of measure, i.e. [s] for time and [m] for length.

The soma is placed on the left of the x semi-axis' origin ($x = 0$) and the tip of the growing axonat $x = l$. As one can easily figure out, l will be a function of time, $l = l(t)$ (which is part of the solution).

In neuronal physiology (see Section 1.4) it is a known fact that the growth of a newborn axon is strictly connected to the presence of a protein known as *tubulin*. Let $c = c(x, t)$ denote the concentration of said protein in the axon.

The growth cone will be idealized as a *completely mixed compartment* sitting at $x = l(t)$. That is to say, the concentration of tubulin in the growth cone is uniform in space and depends only on time. Here is a list of constants and quantities which will be used when describing the axon's structure:

- z: length of the growth cone / mixed compartment; [m]
- A: cross-sectional area of the body of the axon; $\left[\mathrm{m}^2\right]$
- $c_0(t)$: tubulin concentration in the soma, which can in general depend on time; $\left[\frac{\mathrm{kg}}{\mathrm{m}^3}\right]$
- $c_c(t)$: tubulin concentration in the growth cone - does not depend on x. $\left[\frac{\mathrm{kg}}{\mathrm{m}^3}\right]$

Tubulin is produced in the soma, where it is assumed to be present with a concentration c_0 (said concentration will be in general a function of t). It then moves to the growth cone and is in various ways used, as follows.

Tubulin dynamics is composed of two factors: *movement* and *degradation*. Tubulin moves with a certain velocity from the soma to the growth cone, and it might undergo disassembly into its smaller subunits, which are not capable of forming new microtubules. Here are the constants for tubulin dynamics that will be used:

- v: speed of tubulin movement in the axon; $\left[\frac{\mathrm{m}}{\mathrm{s}}\right]$
- g: disassembly rate for tubulin; $\left[\frac{1}{s}\right]$

Note that it is assumed that it is not possible for tubulin to be generated or otherwise rebuilt within the axon itself: all the chemical comes from the soma.

2.2.2 Mass Conservation Law in the Axon

As mentioned before, tubulin moves with a certain velocity v along the length of the axon. The flux of tubulin per area unit in a given interval of space can then be defined as

$$F \stackrel{def}{=} vc.$$

In general F might depend on both space and time, as well as the concentration and/or its gradient:

$$F = F(x, t, c, c_x).$$

It is reasonable in a first moment to assume that in the growing axon a conservation law for the mass of tubulin holds:

$$\frac{\partial c}{\partial t} + F_x = S(c, x, t) \text{ for } 0 < x < l(t), \tag{2.1}$$

where $S(c, x, t)$ contains all the source and sink terms.

Conservation of mass in the growth cone implies another relation. Consider Figure 2.3 the cross interface between the growing axon and the growth cone – flux in is only from the left side. This boundary moves with speed $\frac{dl}{dt}$ while the tubulin moves with (a slightly higher) velocity v, the next flux is

$$Ac(l(t)^-, t)(v - \frac{dl}{dt}),$$

where

$$c(l(t)^-, t) = \lim_{\epsilon \searrow 0} c(l(t) - \epsilon, t).$$

The conservation of mass for the cone leads to the following ODE:

$$\frac{d(V_c c_c)}{dt} = A\left(v|_{x=l} - \frac{dl}{dt}\right) c(l(t)^-, t) \tag{2.2}$$

where $V_c = Az$ is the volume of the growth cone.

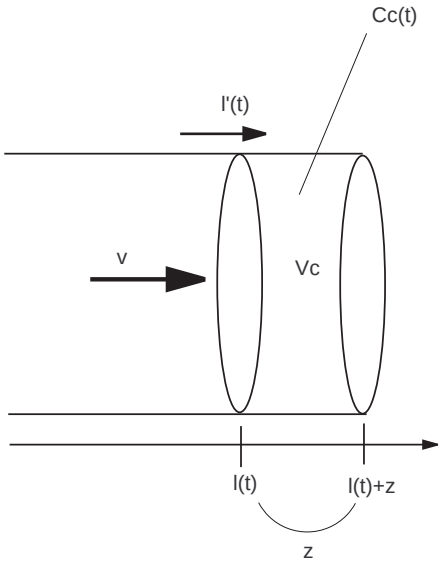

Figure 2.3: Zoom in illustration for a growth cone.

2.2.3 Constitutive Assumptions

The model now has two equations, (2.1) and (2.2) in five unknowns: $c(x,t)$, $c_c(t)$, $l(t)$, F and S. We need some more information if we hope to find a solution for the model. To get this, constitutive assumptions have to be made both concerning the flux of the tubulin in the axon and the elongation of the axon itself.

Constitutive Assumption: Axon

The flux of tubulin, as mentioned, can depend on various elements and be more or less complicated. It will be assumed that the flux is determined given

- the speed a $\left[\frac{\mathrm{m}}{\mathrm{s}}\right]$ of advective transport and
- a diffusion coefficient D $\left[\frac{\mathrm{m}^2}{\mathrm{s}}\right]$,

the flux term is then described as

$$F(c, c_x) = ac - Dc_x.$$

Under this assumption, the following expression holds for the speed of tubulin:

$$v(c, c_x) = \frac{F}{c} = a - D\frac{c_x}{c}.$$

Recall that we assumed no generation of the tubulin along the axon; the source and sink term $S(c,x,t)$ will then only consist of the disassembly term,

$$S(c) = -gc.$$

The Model equations will then be modified in the following ways:

- substituting the expressions for F and S into Equation (2.1) one has

$$\frac{\partial c}{\partial t} + (ac - Dc_x)_x = -gc.$$

With a moment of reflection the final form can be obtained:

$$\frac{\partial c}{\partial t} + a\frac{\partial c}{\partial x} - D\frac{\partial^2 c}{\partial x^2} = -gc. \tag{2.3}$$

This is an *advection-diffusion* equation;

- plugging in the new expression for v in Equation (2.2) yields

$$\begin{aligned} &\frac{d(Azc_c)}{dt} = A\left(\left(a - D\frac{c_x}{c}\right)_{x=l} - \frac{dl}{dt}\right)c(l(t)^-, t) \\ \Rightarrow &z\frac{dc_c}{dt} = ac(l(t)^-, t) - D\left(c_x\frac{c(l(t)^-, t)}{c}\right)_{x=l} - \frac{dl}{dt}c(l(t)^-, t) \\ \Rightarrow &z\frac{dc_c}{dt} = ac(l(t)^-, t) - D\left(c_x\right)_{x=l} - \frac{dl}{dt}c(l(t)^-, t) \end{aligned} \tag{2.4}$$

where c_x should be interpreted as a left derivative in $x = l$ and $c(x, t)$ is again assumed to be smooth enough in $[0, l(t)]$.

Constitutive Assumptions: Growth cone

This model has now three unknowns and two equations: one which explains how the actual elongation occurs is still lacking. This can be provided by considering the connection between increase in building material and usage of tubulin in the cone.

To this end, some new quantities have to be defined. Let:

- A_g be the effective area of growth at the tip of the growth cone; $\left[\mathrm{m}^2\right]$
- ρ the density of built cells in the cone's surface; $\left[\frac{\mathrm{kg}}{\mathrm{m}^3}\right]$
- $\tilde{r}_g$ the assembly rate of the tubulin in the growth cone. $\left[\frac{1}{\mathrm{s}}\right]$

Clearly, the amount of tubulin which is used in the growth cone must be equal to the amount of tubulin which is assembled in the surface to permit growth. Therefore we can write the following equation:

$$\rho A_g \frac{dl}{dt} = \tilde{r}_g A z c_c(t),$$

where the left-hand side is the expression of the amount ot tubulin per unit time used as building material while the right-hand one describes the amount of tubulin lost in the growth cone, under the assumption that this is proportional to the mass (recall $V_c = Az$) in the cone with rate $\tilde{r_g}$.

Simple algebraic manipulation yields the growth equation in its final form:

$$\frac{dl}{dt} = r_g z c_c(t) \tag{2.5}$$

with the new coefficient

$$r_g \overset{def}{=} \frac{\tilde{r}_g A}{\rho A_g}$$

(unit of measure $\left[\frac{m^3}{s \cdot kg}\right]$).

2.2.4 Boundary, Initial Conditions

Now the model has three equations, one PDE and two ODEs. In order for it to be solvable, boundary conditions are needed. Due to the biological setting and the expection for diffusion to be present, continuous boundary conditions are reasonable. For $t > 0$ the following is assumed:

1. $c(0,t) = c_0(t)\ \forall t > 0$ (the concentration of tubulin at the connection point is equal to the concentration in the soma);
2. $c(l,t) = c_c(t)\ \forall t$ (the concentration at the interface with the cone is equal to the one inside).

Using the second condition, it is possible to slightly manipulate Equation (2.4) into:

$$z\frac{dc_c}{dt} = ac_c(t) - Dc_x|_{x=l} - \frac{dl}{dt}c_c(t). \tag{2.6}$$

The following initial conditions are imposed:

$$c(x,0) = c_0(0) \text{ for } 0 < x < l(0) = l_0 \text{ and } c_c(0) = c_0(0).$$

2.2.5 Final Model

Summing up (2.3), (2.6) and (2.5) with the boundary conditions, the complete model for the growth of the axon turns out to be as follows:

$$\begin{cases} \dfrac{\partial c}{\partial t} + a\dfrac{\partial c}{\partial x} - D\dfrac{\partial^2 c}{\partial x^2} = -gc \text{ for } 0 < x < l(t) \\ z\dfrac{dc_c}{dt} = ac_c(t) - Dc_x|_{x=l} - \dfrac{dl}{dt}c_c(t) \text{ for } t > 0 \\ \dfrac{dl}{dt} = r_g z c_c(t),\ t > 0 \\ c(0,t) = c_0(t),\ t > 0 \\ c(l(t),t) = c_c(t),\ t > 0 \\ c(x,0) = c_0(0) \text{ for } 0 < x < l(0) = l_0 \\ c_c(0) = c_0(0) \end{cases}$$

Note that (2.5) can be plugged in (2.6) t to remove one derivative, leading to

$$\begin{cases} \dfrac{\partial c}{\partial t} + a\dfrac{\partial c}{\partial x} - D\dfrac{\partial^2 c}{\partial x^2} = -gc \text{ for } 0 < x < l(t) \\ z\dfrac{dc_c}{dt} = ac_c(t) - Dc_x|_{x=l} - r_g z c_c^2(t) \text{ for } t > 0 \\ \dfrac{dl}{dt} = r_g z c_c(t),\ t > 0 \\ c(0,t) = c_0(0),\ t > 0 \\ c(l(t),t) = c_c(t),\ t > 0 \\ c(x,0) = c_0(0) \text{ for } 0 < x < l(0) = l_0 \\ c_c(0) = c_0(0) \end{cases} \tag{2.7}$$

Chapter 3

Model Study

> Models can easily become so complex
> that they are impenetrable,
> unexaminable, and virtually unalterable.
>
> DONELLA MEADOWS
> *The unavoidable a priori*

In this chapter, the model introduced in Section 2.2.5 will be discussed and studied. Both an (relatively small) analytical and a numerical approach will be attempted. The chapter has the following structure:

- Section 3.1 deals with the non-dimensionalization of the model, to simplify the calculations;
- in Section 3.2 a Steady-State approximation is discussed for the analytical solution;
- Section 3.3 presents two different numerical algorithms to approximate the analytical solutions, one implicit (3.3.1) and one explicit (3.3.2).

3.1 Non-dimensionalization

It is assumed in the previous chapter that all quantities are in SI units of measure. This brings to very small quantities, usually of magnitude 10^{-6} or smaller. In order to obtain quantities of magnitude 1, it is useful to non-dimensionalize all the equations in the model (2.7).

To this end, let

$$\begin{cases} t^* = \dfrac{t}{t_\infty} \\ x^* = \dfrac{x}{l_\infty} \\ c^*(x^*, t^*) = \dfrac{c(x,t)}{c_0(0)} \end{cases}$$

where $c_0(0)$ is again the tubulin concentration in the soma (at time $t = 0$), t_∞ is the average growth time of a squid axon and l_∞ is the average length of a full grown squid giant axon. As a direct consequence of this transformation, we also have another one:

$$l^* = \frac{l}{l_\infty}.$$

We shall now transform all the equations in (2.7) using these new variables. The non-dimensionalized form of Equation (2.3) is:

$$\frac{c_0}{t_\infty}\frac{\partial c^*}{\partial t^*} + \frac{ac_0}{l_\infty}\frac{\partial c^*}{\partial x^*} - \frac{Dc_0}{(l_\infty)^2}\frac{\partial^2 c^*}{\partial (x^*)^2} = -gc_0c^*;$$

with some simple algebra and dropping the asterisks we get

$$\frac{\partial c}{\partial t} + \frac{at_\infty}{l_\infty}\frac{\partial c}{\partial x} - \frac{Dt_\infty}{(l_\infty)^2}\frac{\partial^2 c}{\partial x^2} = -gt_\infty c.$$

Let

- $\alpha = \frac{at_\infty}{l_\infty}$, ratio between the average distance travelled by the particles due to active transport and the length of the full grown axon;
- $Fo_m = \frac{Dt_\infty}{(l_\infty)^2}$, often called the *Mass Fourier Number*;
- $\eta = gt_\infty$, a measure of the amount of tubulin particles that meet disassembly over the course of the growth.

We can then write down the final form for the nondimensionalized first equation:

$$\frac{\partial c}{\partial t} + \alpha\frac{\partial c}{\partial x} - Fo_m\frac{\partial^2 c}{\partial x^2} = -\eta c. \tag{3.1}$$

Non-dimensionalization of Equation (2.6) yields the following result:

$$\begin{aligned} \frac{dc_c^*}{dt^*} &= \frac{at_\infty}{l_\infty z^*}c_c^* - \frac{Dt_\infty}{z^* l_\infty^2}\frac{\partial c^*}{\partial x^*}|_{x=l} - \frac{1}{z^*}\frac{dl^*}{dt^*}c_c^* \\ \Rightarrow \frac{dc_c^*}{dt^*} &= \frac{\alpha}{z^*}c_c^* - \frac{Fo_m}{z^*}\frac{\partial c^*}{\partial x^*}|_{x=l} - \frac{1}{z^*}\frac{dl^*}{dt^*}c_c^* \end{aligned}$$

where $z^* = \frac{z}{l_\infty}$.

The non-dimensionalized second equation states as follows (again dropping all asterisks):

$$\frac{dc_c}{dt} = \frac{\alpha}{z}c_c - \frac{Fo_m}{z}\frac{dc}{dx} - \frac{1}{z}\frac{dl}{dt}c_c. \tag{3.2}$$

Applying the non-dimensionalizing transformation to the third equation (2.5) yields:

$$\frac{dl^*}{dt^*} = r_g t_\infty c_0 z^* c_c^*;$$

defining

$$r_g^* = r_g t_0 c_0$$

and dropping asterisks as usual we get

$$\frac{dl}{dt} = r_g z c_c(t); \tag{3.3}$$

Non-dimensionalizing the boundary conditions of (2.7) leads to:

$$\begin{cases} c^*(0,t^*) = 1 \\ c^*(l^*(t),t^*) = c_c^*(t) \end{cases} \tag{3.4}$$

while the initial conditions transform this way:

$$\begin{cases} c^*(x^*,0) = 1 \text{ for } 0 < x^* < l^*(0) = l_0^* \\ c_c^*(0) = 1 \end{cases} \tag{3.5}$$

where $l_0^* = \frac{l_0}{l_\infty}$. The new, non-dimensionalized PDE model we will use is then defined as follows:

$$\begin{cases} \dfrac{\partial c}{\partial t} + \alpha \dfrac{\partial c}{\partial x} - Fo_m \dfrac{\partial^2 c}{\partial x^2} = -\eta c \text{ for } 0 < x < 1 \\ \dfrac{dc_c}{dt} = \dfrac{\alpha}{z} c_c - \dfrac{Fo_m}{z} \dfrac{\partial c}{\partial x}|_{x=l} - r_g \ z \ c_c^2 \text{ for } t > 0 \\ \dfrac{dl}{dt} = r_g z c_c(t) \text{ for } t > 0 \\ c(0,t) = 1 \\ c(l(t),t) = c_c(t) \\ c(x,0) = 1 \text{ for } 0 < x < l(0) = l_0 \\ c_c(0) = 1 \end{cases} \tag{3.6}$$

3.2 Steady-State solution

Biologically, a *Steady-State* (from here on SS) solution corresponds to the concentration of tubulin in a full grown axon, that has latched to its target neuron.[1] From a mathematical point of view, imposing the SS condition means assuming all functions to be indipendent of time. From this assumption we immediately obtain

$$\frac{dl}{dt} = 0 \Rightarrow l(t) = l_\infty,$$

where l_∞ can be thought of as the length of the full grown axon. This quantity is unknown and must be determined by solving the (SS) model itself.

Equation (3.3) then assumes the following form:

$$0 = r_g \ z \ c_c(t) \Rightarrow c_c(t) = 0;$$

in other words, there is no more tubulin in the growth cone. From a biological point of view, this is explained by noting that there is no more growth cone when the axon is fully grown and has reached its target synapsis. However, in our model we still retain a quantity $z > 0$ a constant. This is due to limitations of the model.

Plugging in the new values in Equations (3.2) yields

$$0 = 0 - Fo_m^z \frac{dc}{dx} - 0 \Rightarrow \frac{dc}{dx}|_{x=l_\infty} = 0.$$

Since everything is now time independent, Equation (3.1) also changes in the following way:

$$\begin{aligned} &\alpha \frac{dc}{dx} - Fo_m \frac{d^2 c}{dx^2} = -\eta c \\ \Rightarrow &Fo_m \frac{d^2 c}{dx^2} - \alpha \frac{dc}{dx} - Nc = 0. \end{aligned}$$

The new model for the SS approximation can be written as follows:

$$\begin{cases} Fo_m \dfrac{d^2 c}{dx^2} - \alpha \dfrac{dc}{dx} - \eta c = 0. \\ c(0) = 1 \\ c(l_\infty) = 0 \\ \dfrac{dc}{dx}|_{x=l_\infty} = 0. \end{cases} \tag{3.7}$$

[1] It is reasonable to assume that a well-defined model should allow for a SS solution to be found, accounting for the full-grown axon. However, this is not the case for our model, as we will show.

The first equation is a second-order linear ODE in $c(x)$. To derive the solution, the following *ansatz* can be made:

$$c(x) = e^{\lambda x}$$

for some $\lambda \in \mathbb{R}$. This yields

$$Fo_m \lambda^2 e^{\lambda x} - \alpha \lambda e^{\lambda x} - \eta e^{\lambda x} = 0,$$

which can easily be reduced to the following algebraic equation for λ:

$$Fo_m \lambda^2 - \alpha \lambda - \eta = 0.$$

For the moment let $Fo_m > 0$. Then the solutions for this second-order equation are:

$$\lambda_{1,2} = \frac{\alpha}{2Fo_m} \pm \sqrt{\left(\frac{\alpha}{2Fo_m}\right)^2 + \frac{\eta}{Fo_m}}.$$

Note that the discriminant $\left(\frac{\alpha}{2Fo_m}\right)^2 + \frac{\eta}{Fo_m}$ is non-negative due to the limitations on the parameters. This implies the existence of both the real roots λ_1 and λ_2: the general solution can then be written using the linearity of the ODE as

$$c(x) = k_1 e^{\lambda_1 x} + k_2 e^{\lambda_2 x} \tag{3.8}$$

for some $k_1, k_2 \in \mathbb{R}$ to be found.

Our model now has three distinct unknowns: k_1, k_2 and l_∞. Conveniently, the system (3.7) has three equations which can be used to extract this values. Substituing (3.8) in the model and running through the easy math we get to the following system for k_1, k_2, l_∞:

$$\begin{cases} k_1 + k_2 = 1 \\ k_1 e^{\lambda_1 l_\infty} + k_2 e^{\lambda_2 l_\infty} = 0 \\ k_1 \lambda_1 e^{\lambda_1 l_\infty} + k_2 \lambda_2 e^{\lambda_2 l_\infty} = 0. \end{cases}$$

Now several things might happen, depending on the values of $\lambda_{1,2}$:

- $\lambda_1 = 0$: in this case either $k_2 = 0$ or $\lambda_2 = 0$ from the third equation. If $k_2 = 0$, from the first equation we know that $k_1 = 1$, which makes the second equation unsolvable; if instead $\lambda_2 = 0$, the first and second equations are incompatible. Therefore it has to be that $\lambda_1 \neq 0$;
- with an argument of symmetry, it is possible to derive that also $\lambda_2 \neq 0$ must hold;
- if both λ_1 and λ_2 are nonzero, then by multiplying the second equation by a factor λ_1 and subtracting it from the third one can obtain

$$k_2(\lambda_1 - \lambda_2) e^{\lambda_2 l_\infty} = 0;$$

- again, two alternatives: either $\lambda_1 = \lambda_2$ or $k_2 = 0$. k_2 cannot be zero for the same argument as above; if $\lambda_1 = \lambda_2$, using the second equation and cancelling $e^{\lambda_2 x}$ the system is again incompatible.

To conclude the discussion on the steady state approach, let now $Fo_m = 0$. Under this assumption the first equations of (3.7) is reduced to a Malthusian first-order ODE,

$$\frac{dc}{dx} = -\frac{N}{\alpha} c(x),$$

for which the solution is well known:

$$c(x) = ke^{-\frac{\eta}{\alpha}x}.$$

Note that this solution must again fulfill the border conditions of (3.7). From the first one we obtain

$$k = 1,$$

but clearly the second one can never be fulfilled, for the well-known properties of the exponential functions. So this system does not have a SS solution *at all*.

The biological reason underlying this result could be found in the fact that this model assumes a constant production of tubulin in the soma. Since the elongation from the soma is directly proportional to the presence of tubulin, in this idelization the axon can never stop growing, hence there can be no solution of this kind.

3.3 Numerical Approach

As it often happens when dealing with PDE models, an exact analytical solution is very hard to find, not to mention compute for all couples (x, t). To address this, a numerical approach has been undertaken, seeking an appropriate approximation of the true solution $c(x, t)$. The description of this approach is in the following.

3.3.1 A Semi-Implicit Euler Algorithm

Consider the interval $[0, t_\infty]$ and consider a partition of said interval into N subintervals each of length $\Delta t \stackrel{def}{=} \frac{t_\infty}{N}$; this yields the following time mesh:

$$\mathcal{T}_N \stackrel{def}{=} \{t_n, n = 0, \dots N \mid t_n = n\Delta t\}.$$

For each time step t_n, a space mesh is needed to solve the PDE and the first ODE. However, one cannot simply impose a uniform and time-independent mesh: this is due to the fact that the domain of integration changes with time, and in a non-uniform way (i.e. the axon can in theory grow with different speed at different times).

To solve this problem, a constructive method has been developed, as follows.

3.3.2 Spatial Mesh, Discrete Functions

From the construction of the model, it appears that at each time step Δt the axon increases its length of a certain amount, which as mentioned can be time-dependent. Let, for each n, Δx_n be said amount. Let also

$$L_n \approx l(t_n)$$

be the total length of the axon at time t_n. It follows immediately from what has been said that

$$L_n = \sum_{i=0}^{n} \Delta x_i.$$

Assuming that the axon elongates from a starting point $x_0 = 0$ where the connection with the soma is located, a spatial mesh at time point n can be defined as follows:

$$\mathcal{X}_n \stackrel{def}{=} \{x_0 = 0\} \cup \left\{ x_j, j = 1, \dots, n+1 \mid x_j = \sum_{k=0}^{j} \Delta x_k \right\} \cup \{L_n + z\}$$

where the last element represents the growth cone's maximum extension at the tip of the axon.

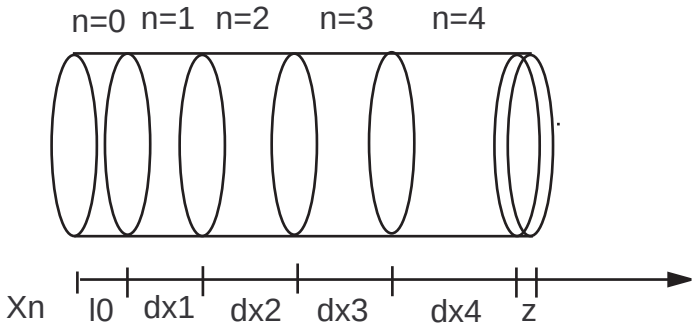

Figure 3.1: Progressive building of the space mesh. Time is increasing with n.

This mesh also defines a sequence of "cells", which extend from one space point to the following. At time step t_n the cells are in number of $n+1$, and cell number $j \in 0, \ldots, n$ can be represented with the space interval $[x_j, x_{j+1}]$.

Let now $C_{j,n}$ be the concentration of tubulin at time t_n in cell j. This is a simple function over the grid

$$\mathcal{M}_n = \mathcal{X}_n \times \mathcal{T}_N$$

that approximates the $(\mathcal{C}^2)$ concentration function $c(x,t)$.

Let finally C_c^n be the concentration of tubulin in the growth cone mixed compartment at time t_n.

3.3.3 Discrete Equations, Algorithm

Recall the equation in System (3.6). The goal is now to produce a numerical, possibly iterative algorithm to solve this system for variables $C_{j,n}, L_n, C_c^n$ on the grid $\mathcal{M}_n$. To achieve this, an Implicit (backward) Euler method will be used for the PDE while an Explicit (Forward) method will be applied on the two ODEs (for the time stepping). To approximate the derivatives, a Finite Difference scheme has been implemented. In the specific case of the spatial partial derivative, the first order derivation is computed on the mean points of the intervals Δx_j.

Therefore the following approximations have been imposed for the first order space and time derivatives:

$$\frac{\partial c}{\partial t}(x_j, t_n) \approx \frac{C_{j,n+1} - C_{j,n}}{\Delta t};$$
$$\frac{\partial c}{\partial x}(x_j, t_n) \approx \frac{C_{j,n} - C_{j-1,n}}{\frac{\Delta x_j + \Delta x_{j-1}}{2}};$$

In order to simplify reading let for all $j = 1, \ldots, n$

$$\lambda_j \stackrel{def}{=} 2\frac{\Delta t}{\Delta x_j + \Delta x_{j-1}}.$$

This allows one to rewrite:

$$\Delta t \frac{\partial c}{\partial x}(x_j, t_n) \approx \lambda_j \left(C_{j,n} - C_{j,n-1}\right)$$

as well as

$$\Delta t \frac{\partial^2 c}{\partial x^2} \approx \frac{\Delta t}{\Delta x_j}\left(2\frac{C_{j+1,n} - C_{j,n}}{\Delta x_{j+1} + \Delta x_j} - 2\frac{C_{j,n} - C_{j-1,n}}{\Delta x_j + \Delta x_{j-1}}\right) =$$
$$= \frac{1}{\Delta x_j}\left[\lambda_{j+1}(C_{j+1,n} - C_{j,n}) - \lambda_j(C_{j,n} - C_{j-1,n})\right]$$

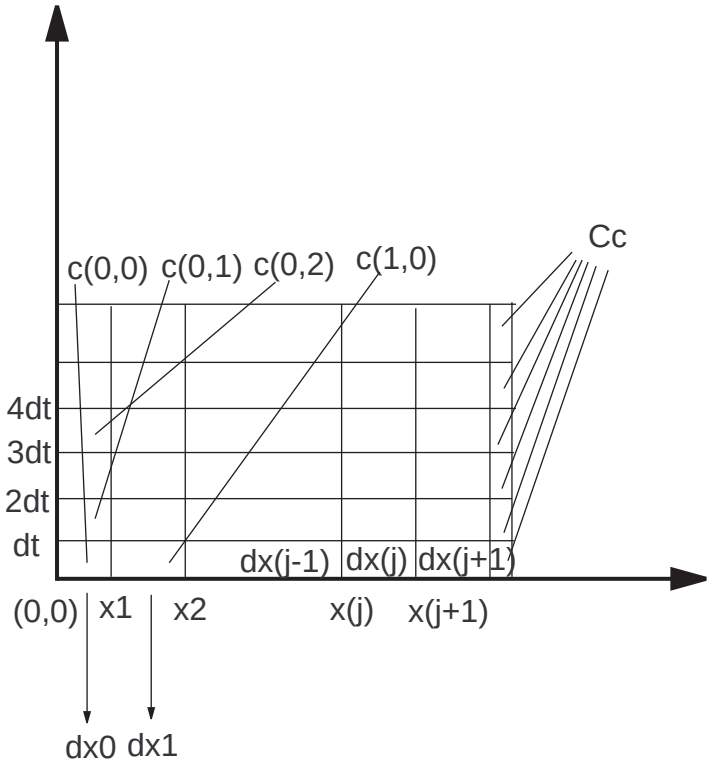

Figure 3.2: Example of an $\mathcal{M}_n$ grid.

Now the tools are ready to discretize the equations in model (3.6). To begin with, applying the forward Euler method as mentioned to the third equation one obtains:

$$\begin{aligned} \frac{L_{n+1} - L_n}{\Delta t} &= r_g \; z \; C_c^n; \\ \Rightarrow L_{n+1} &= L_n + \Delta t \; r_g z \; C_c^n \end{aligned} \tag{3.9}$$

solving this equation at time t_n yields the axon length at time t_{n+1}, L_{n+1}. One can also calculate the new increment / spatial step using

$$\Delta x_{n+1} = L_{n+1} - L_n.$$

With this new values it is possible to compute the next cone concentration by using the second equation:

$$\frac{C_c^{n+1} - C_c^n}{\Delta t} = \frac{\alpha}{z} C_c^n - \frac{Fo_m}{z} \frac{\lambda_n}{\Delta t} (C_{n,n} - C_{n-1,n}) - r_g \frac{z}{z} (C_c^n)^2$$

Moving around the terms and multiplying by Δt, one obtains:

$$C_c^{n+1} = \left(1 + \frac{\alpha \Delta t}{z} - r_g \Delta t C_c^n\right) C_c^n - \frac{Fo_m}{z} \lambda_n \left(C_{n,n} - C_{n,n-1}\right). \tag{3.10}$$

This step is mandatory to obtain one of the two boundary conditions for the PDE. To complete one iteration of the loop it is necessary to update the inner cells using the PDE in (3.6). This is where the implicit Euler is used. The discretized PDE looks like this:

$$\begin{aligned} &\frac{C_{j,n+1} - C_{j,n}}{\Delta t} + \alpha \frac{\lambda_j}{\Delta t} (C_{j,n+1} - C_{j-1,n+1}) - \\ &- \frac{Fo_m}{\Delta x_j \Delta t} \left[\lambda_{j+1} (C_{j+1,n+1} - C_{j,n+1}) - \lambda_j (C_{j,n+1} - C_{j-1,n+1})\right] = -\eta C_{j,n+1}. \end{aligned}$$

for $j = 0, \ldots, n-1$ at a fixed time t_n, $n \geq 2$. As it goes when solving implicit Euler equations, it is convenient to transform this system of equations to a different form. To do that, some rearrangements are in order. To begin with, explicitating the coefficients, multiplying by a factor Δt and rearranging for j yields:

$$\begin{aligned} &\left(-\alpha\lambda_j - \frac{Fo_m\lambda_j}{\Delta x_j}\right) C_{j-1,n+1} + \\ &+ \left[1 + \alpha\lambda_j + \frac{Fo_m}{\Delta x_j}(\lambda_{j+1} + \lambda_j) + \eta\Delta t\right] C_{j,n+1} + \\ &+ \left(-\frac{Fo_m}{\Delta x_j}\lambda_{j+1}\right) C_{j+1,n+1} = C_{j,n} \end{aligned} \tag{3.11}$$

for $j = 1, \ldots, n$ at a fixed time $t_n = n\Delta t$.

Let for the sake of convenience,

$$\begin{aligned} A_{-1}^j &\stackrel{def}{=} -\alpha\lambda_j - \frac{Fo_m\lambda_j}{\Delta x_j} \\ A_0^j &\stackrel{def}{=} 1 + \alpha\lambda_j + \frac{Fo_m}{\Delta x_j}(\lambda_{j+1} + \lambda_j) + \eta\Delta t \\ A_{+1}^j &\stackrel{def}{=} -\frac{Fo_m}{\Delta x_j}\lambda_{j+1} \end{aligned}$$

and $A \in M_{n\times n}(\mathbb{R})$ be matrix used to represent Equation (3.11) (for $n \geq 2$). Then A can be written as:

$$\begin{pmatrix} A_0^1 & A_{+1}^1 & 0 & 0 & \ldots & 0 \\ A_{-1}^2 & A_0^2 & A_{+1}^2 & 0 & \ldots & 0 \\ 0 & A_{-1}^3 & A_0^3 & A_{+1}^3 & \ldots & 0 \\ \vdots & \vdots & \vdots & \vdots & \ddots & \vdots \\ 0 & 0 & \ldots & 0 & A_{-1}^n & A_0^n \end{pmatrix}$$

To finalize the system,, one must make sure that the boundary conditions

$$C_{0,n+1} = 1,\ C_{n+1,n+1} = C_c^{n+1}.$$

are imposed. To address this, compare first that the equation that one obtains by choosing $j = 1$, i.e.

$$A_{-1}^1 C_{0,n+1} + A_0^1 C_{1,n+1} + A_{+1}^1 C_{1,n+1} = C_{1,n}$$

with the equation which is obtained by considering only the terms from the first row of A:

$$A_0^1 C_{1,n+1} + A_{+1}^1 C_{1,n+1} = C_{1,n}$$

The term with index -1 do not appear in the linear system, but it should be there, as it is part of the equations. In fact, that terms keeps into account the effect of the left boundary condition: they are already known due to the equations in Section 2.4, and so they do not need to be computed. A similar reasoning shows the lack of a right boundary condition term in the last row of the system (term for $j = n-1$, missing $A_{+1}^n C_{n+1,n+1}$). As mentioned, it is known that $C_{0,n+1} = 1$ and $C_{n+1,n+1} = C_c^{n+1}$, so the two missing terms are in fact known terms - scalar numbers that can be computed. Consider for example the following systems of equations at time step $n = 3$:

$$\begin{cases} \underline{A_{-1}^1 C_{0,4}} + A_0^1 C_{1,4} + A_1^1 C_{2,4} = C_{1,3} \\ A_{-1}^2 C_{1,4} + A_0^2 C_{2,4} + A_1^2 C_{3,4} = C_{2,3} \\ A_{-1}^3 C_{2,4} + A_0^3 C_{3,4} + \underline{A_1^3 C_{4,4}} = C_{3,3} \end{cases}$$

The underlined terms are scalar, known terms that can be moved to the right-hand side, yielding:

$$\begin{cases} A_0^1 C_{1,4} + A_1^1 C_{2,4} = C_{1,3} - \underline{A_{-1}^1 C_{0,4}} \\ A_{-1}^2 C_{1,4} + A_0^2 C_{2,4} + A_1^2 C_{3,4} = C_{2,3} \\ A_{-1}^3 C_{2,4} + A_0^3 C_{3,4} = C_{3,3} - \underline{A_1^3 C_{4,4}} \end{cases}$$

Now define the following:

$$A^{(3)} = \begin{pmatrix} A_0^1 & A_1^1 & 0 \\ A_{-1}^2 & A_0^2 & A_1^2 \\ 0 & A_{-1}^3 & A_0^3 \end{pmatrix}$$

and

$$B = \begin{pmatrix} A_{-1}^1 C_{0,4} \\ 0 \\ A_1^3 C_{4,4} \end{pmatrix}.$$

Then the concentration of tubulin at the next time step can be found by solving

$$A^{(3)} \begin{pmatrix} C_{1,4} \\ C_{2,4} \\ C_{3,4} \end{pmatrix} = \begin{pmatrix} C_{1,3} \\ C_{2,3} \\ C_{3,3} \end{pmatrix} - B.$$

To extend to the general case above, one could simply define

$$B = \begin{pmatrix} A_{-1}^1 C_{0,n+1} \\ 0 \\ \dots \\ 0 \\ A_1^{n+1} C_{n+1,n+1} \end{pmatrix};$$

this vector always contains $n-2$ null entries. Let then

$$b_n \stackrel{def}{=} \begin{pmatrix} C_{1,n} \\ C_{2,n} \\ \vdots \\ \vdots \\ C_{n-1,n} \end{pmatrix} - B$$

and

$$\Gamma_n \stackrel{def}{=} \begin{pmatrix} C_{1,n} \\ C_{2,n} \\ \vdots \\ \vdots \\ C_{n-1,n} \end{pmatrix}.$$

One can then write the final form of the discrete PDE:

$$A\Gamma_{n+1} = b_n, \tag{3.12}$$

where Γ_{n+1} is unknown and b_n is known. This can be solved using a preferred linear system solving algorithm. Note that the A matrix is always tridiagonal (courtesy of the method used) and for large values of n it becomes sparse.

It can be observed that this procedure is inconsistent for the values $n = 0, 1$: in the former case there is no internal intervals and thus no PDE needs to be solved; in the latter, the b vector assumes a different form (due to the presence of only one internal interval).

To further simplify the understanding of how this algorithm works, the calculation for cases $n = 0, 1$ and 2 have been reported. This is done under the assumptions that c_0 is constant for all t. Assume all parameters to be known and already set.

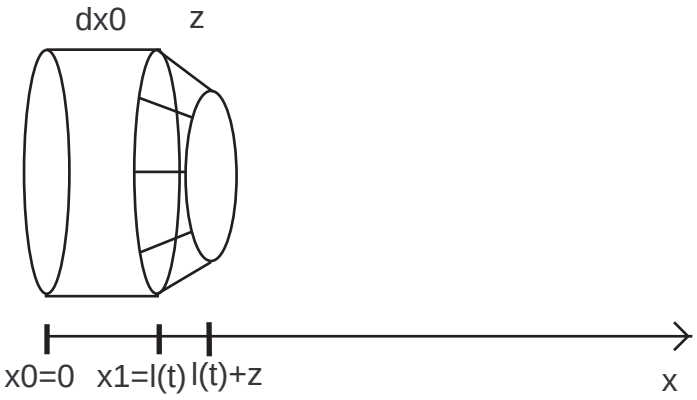

Figure 3.3: Initial state of the system.

$$n = 0$$

The system in the initial condition. This iteration is particular, in the sense that there is no PDE so solve, as everything is fixed by the boundary conditions.

1. $L(1) = l_0 + \Delta t \; r_g \; z \; C_c(0)$;
2. $\Delta x(1) = L(1) - l_0$;
3. There is no λ calculation at this stage, since there is no "internal" points;
4. $C_c(1) = \left(1 + \frac{\alpha \Delta t}{z} - r_g \; \Delta t \; C_c(0)\right) C_c(0)$. There is no term concerning the right concentration at $x = L(t)$ for the aforementioned reasons;
5. $C_{0,1} = 1, \; C_{1,1} = C_c(1)$;
6. No construction of matrix A since no PDE needs to be solved.

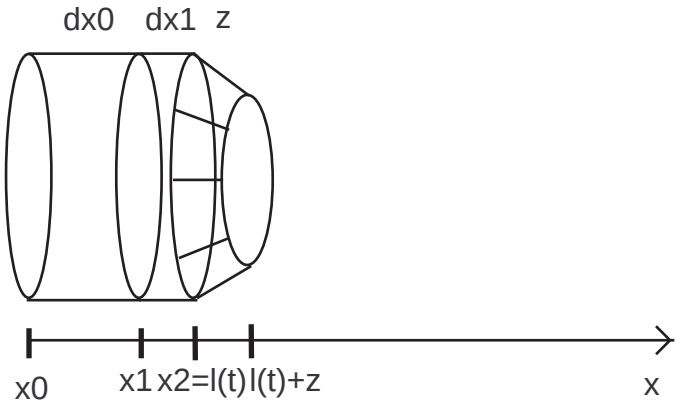

Figure 3.4: Snapshot at the start of iteration 1. The axon is starting to be built.

$$n = 1$$

Beginning iteration 1. Now there will be at least one internal segment to be dealt with, so the algorithm will run fully.

1. $L(2) = L(1) + \Delta t\ r_g\ z\ C_c(1)$;
2. $\Delta x(2) = L(2) - L(1)$;
3. $\lambda_1 = 2\frac{\Delta t}{\Delta x_1 + \Delta x_0}$,
   $\lambda_2 = 2\frac{\Delta t}{\Delta x_2 + \Delta x_1}$,
4. $C_c(2) = \left(1 + \frac{\alpha \Delta t}{z} - r_g\ \Delta t\ C_c(1)\right) C_c(1) - \frac{Fo_m}{z} \lambda_1 (C_{1,1} - C_{1,0})$;
5. $C_{0,2} = 1,\ C_{2,2} = C_c(2)$;
6. $A_0^1 = 1 + \alpha\lambda_1 + \frac{Fo_m}{z}(\lambda_2 + \lambda_1) + \eta\Delta t$;
7. $A = \left[A_0^1\right]$. The matrix is a real number;
8. $B = \left(-\alpha\lambda_1 - \frac{Fo_m \lambda_1}{\Delta x_1}\right) c_0 + \left(-\frac{Fo_m}{\Delta x_1}\lambda_2\right) C_c(2)$. The B vector is also reduce to a scalar in this iteration;
9. $\Gamma_{n+1} = A^{-1}\left(\Gamma_n - BC\right)$;

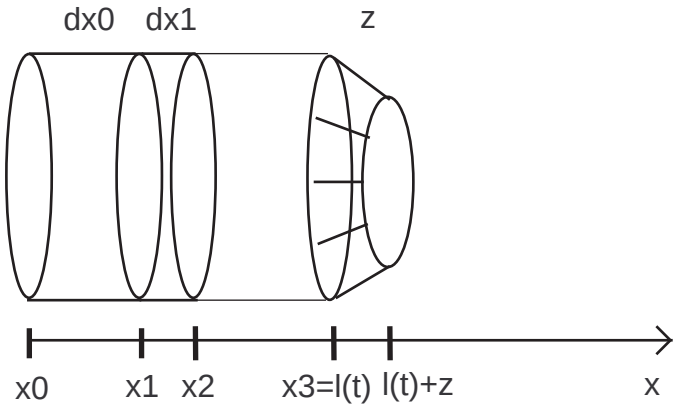

Figure 3.5: Snapshot at the start of iteration 2 (general case).

$$n = 2$$

Beginning iteration 2.

1. $L(3) = L(2) + \Delta t\ r_g\ z\ C_c(2)$;
2. $\Delta x(3) = L(3) - L(2)$;
3. $\lambda_3 = 2\frac{\Delta t}{\Delta x_3 + \Delta x_2}$. The other values of lambda can be saved from the preceding iteration;
4. $C_c(3) = \left(1 + \frac{\alpha \Delta t}{z} - r_g\ \Delta t\ C_c(2)\right) C_c(2) - \frac{Fo_m}{z}\lambda_2(C_{2,2} - C_{2,1})$;
5. $C_{0,3} = 1,\ C_{3,3} = C_c(3)$;
6. $A^1_{+1} = -\frac{Fo_m}{\Delta x_1}\lambda_2$;
   $A^2_0 = 1 + \alpha\lambda_2 + \frac{Fo_m}{z}(\lambda_3 + \lambda_2) + \eta\Delta t$;
   $A^2_{-1} = -\alpha\lambda_2 - \frac{Fo_m\lambda_2}{\Delta x_2}$;
7. $A = \begin{pmatrix} A^1_0 & A^1_{+1} \\ A^2_{-1} & A^2_0 \end{pmatrix}$;
8. $B = \begin{pmatrix} \left(-\alpha\lambda_1 - \frac{Fo_m\lambda_1}{\Delta x_1}\right) c_0 \\ \left(-\frac{Fo_m}{\Delta x_2}\lambda_3\right) C_c(3) \end{pmatrix}$;
9. $\Gamma_{n+1} = A^{-1}\left(\Gamma_n - B\right)$;

3.3.4 Pseudocode

In the following (pseudo)code a procedure for computing the numerical solution is summarized.

An algorithm has been developed to solve this discrete model. The software that has been used is Matlab$^{\mathrm{TM}}$. The script can be found in Appendix A.

Algorithm 1 Pseudo code for solving the PDE-ODE Axon Growth Problem, main loop.

$\Delta t \leftarrow \frac{T}{N}$
$L(0) \leftarrow l_0$
$\Delta x(0) \leftarrow l_0$
for $n = 0 \rightarrow N-1$ **do**
  $L(n+1) \leftarrow L(n) + \Delta t \; r_g \; z \; C_c(n)$
  $\Delta x(n+1) = L(n+1) - L(n)$
  for $j = 1 \rightarrow n+1$ **do**
    $\lambda_j \leftarrow 2\frac{\Delta t}{\Delta x_j + \Delta x_{j-1}}$
  end for
  $C_c(n+1) \leftarrow \left(1 + \frac{\alpha \Delta t}{z} - r_g \Delta t C_c^n\right) C_c^n - \frac{Fo_m}{z}\lambda_n \left(C_{n,n} - C_{n,n-1}\right)$
  $C_{0,n+1} \leftarrow 1$
  $C_{n+1,n+1} \leftarrow C_c(n+1)$
  for $j = 1 \rightarrow n$ **do**
    $A_0^j \leftarrow 1 + \alpha\lambda_j + \frac{Fo_m}{\Delta x_j}(\lambda_{j+1} + \lambda_j) + \eta\Delta t$
    if $j \neq n$ **then**
      $A_{+1}^j \leftarrow -\frac{Fo_m}{\Delta x_j}\lambda_{j+1}$
    end if
    if $j \neq 1$ **then**
      $A_{-1}^j \leftarrow -\alpha\lambda_j - \frac{Fo_m \lambda_j}{\Delta x_j}$
    end if
  end for
  $A \leftarrow \mathrm{diag}(A_0, 0) + \mathrm{diag}(A_{+1}, +1) + \mathrm{diag}(A_{-1}, -1)$
  $BCV(1) \leftarrow \left(-\alpha\lambda_1 - \frac{Fo_m\lambda_1}{\Delta x_1}\right) \cdot 1$
  $BCV(n) \leftarrow \left(-\frac{Fo_m}{\Delta x_n}\lambda_{n+1}\right) C_c^{n+1}$
  $C(\cdot, n+1) \leftarrow A \setminus (C(\cdot, n) - BCV)$
end for

Chapter 4

Experiments and Results

> I am very conscious that there is no scientific explanation for the fact that we are conscious.
>
> Sir ANDREW HUXLEY
> *Quoted in "The Economist"*

In this final chapter, the convergence of the implicit method will be discussed, and a series of tests will be presented where the model's sensitivity to changes in parameter values is put to the test. The Chapter is structured as follows:

- Section 4.1 deals with the parameter values used for the simulations, as well as with explaning how the results will be presented;
- In Section 4.2 a convergence study is conducted to discuss the convergence of the implicit method as $\Delta t \to 0$;
- In Section 4.3 the model is tested with various changes to the paramters, in order to evaluate its sensibility. Specifically,
  1. the initial length of the axon, l_0 (Section 4.3.1),
  2. the growth cone's length, z (Section 4.3.2),
  3. the rate of tubulin assembly in the growth cone, r_g (Section 4.3.3);
  4. the tubulin income as a function of time, $c_0(t)$ (Section 4.3.4);
- Section 4.4 will sum up all the results and knowledge extracted from the analysis;
- Section 4.5 will provide some insight on what else could be done with the model and what further developments can be undertaken.

4.1 Parameter Values. Concentration Plots

As discussed previously in Chapter 2, the model is dependent on the following set of parameters:

- growth cone length z [m];
- initial length of the axon l_0 [m];
- disassembly rate of tubulin g $\left[\frac{1}{\text{s}}\right]$;
- magnitude of tubulin concentration in the soma c_0 $\left[\frac{\text{kg}}{\text{m}^3}\right]$;

Parameter name	*Value*	*Source*
z	$3 - 4\mu\text{m}$	*Assumption*
l_0	***	***
g	$\frac{1}{33*3600}\ \frac{1}{\text{s}}$	[MC02]
c_0	$2 * 10^{-6}\ \frac{\text{kg}}{\text{m}^3}$	[LVDW80]
a	$3.6980 \cdot 10^{-11} \frac{\text{m}}{\text{s}}$	[JAG99]
D	$8.6 \cdot 10^{-12} \frac{\text{m}^2}{\text{s}}$	[JAG99]
r_g	$30 \frac{\text{m}^3}{\text{s}\cdot\text{kg}}$	*Assumption*

Table 4.1: Values for parameters in the numericals simulation of the axonal growth model. Note that the value l_0 was extimated using the first iteration of the code itself: $l_0 \leq c_0(0)\ r_g\ z\ \Delta t$. Also note that the value of a was obtained indirectly using the Péclet number $Pe = 0.86$ found in [JAG99].

- speed of advective transport $a\ \left[\frac{\text{m}}{\text{s}}\right]$;
- diffusion coefficient $D\ \left[\frac{\text{m}^2}{\text{s}}\right]$;
- microtubule assembly rate constant $r_g\ \left[\frac{\text{m}^3}{\text{s}\cdot\text{kg}}\right]$.

Values of these paramaters appear to be fairly hard to find for *Loligo Pealeii*, let alone for humans, so the author was required to assume some of these values using images of squids or other animal data. In Table 4.1 the values used in the computation can be found, along with their source, where available. This set of parameter will be taken as *standard values* for the simulation in all this chapters. In the following sections, one or more of these paramaters can be modified to study the reactions of the model.

Running the algorithm with the standard set of parameters yields the following plots for C, C_c and L:

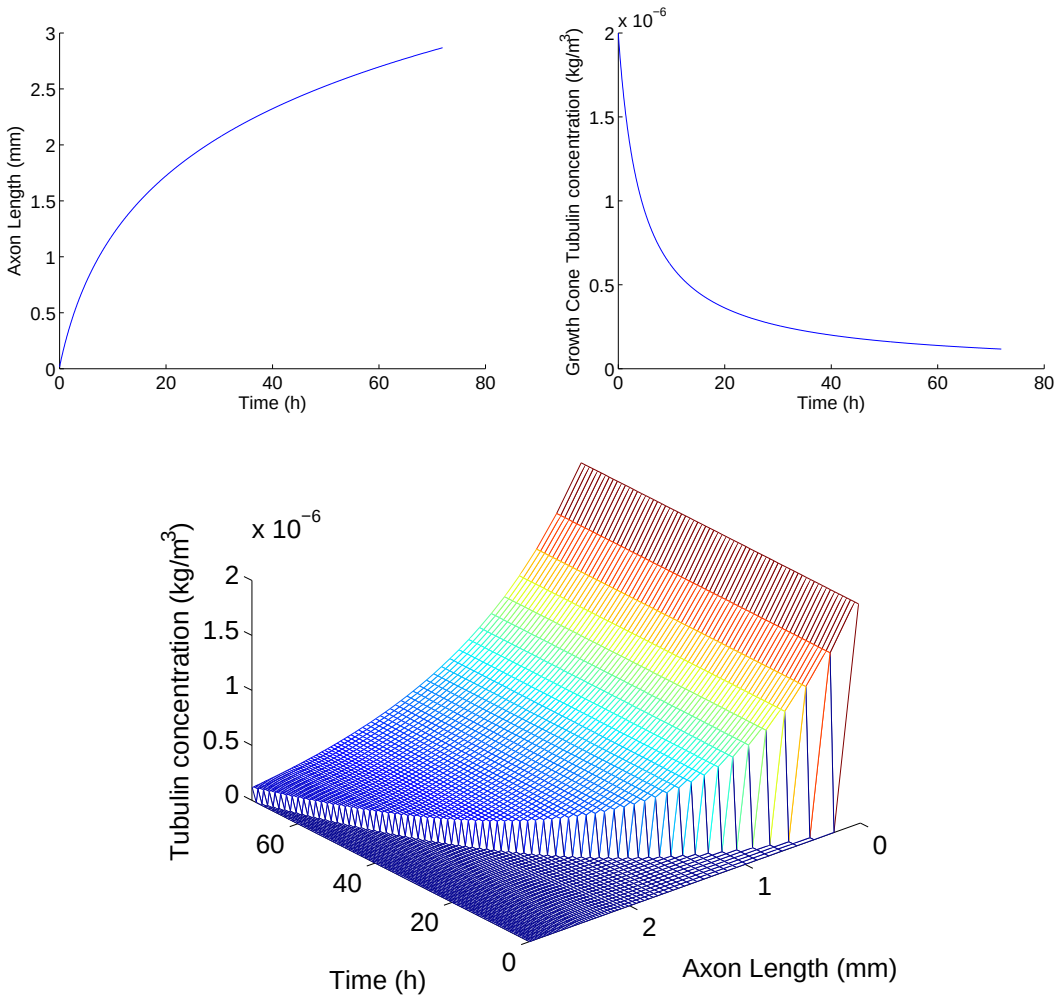

Figure 4.1: Algorithm's results for standard values. (Top-Left) Axon Length with respect to time; (Top-Right) Cone Concentration as a function of time. (Center) Three-dimensional plot of tubulin concentration with respect to time and space. For visibility, coarser mesh sizes have been chosen for the 3D graph than the ones used in the calculations.

4.2 Convergence Study

Convergence tests have been run on the standard-valued algorithm. These tests consist in sequential runs of the algorithm with progressively decreasing values of Δt. Results for both $l(t)$ and $C_c(t)$ values are shown in Figure 4.2. The plots highlight what seems to be a pretty smooth convergence of the code.

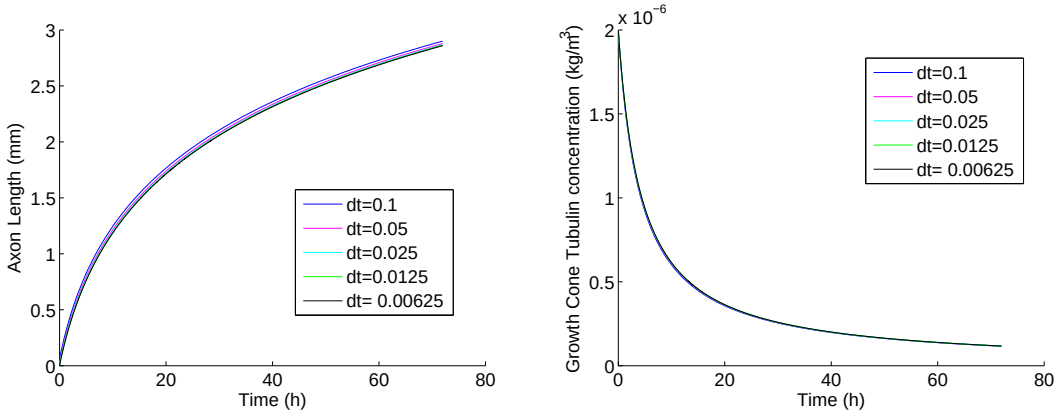

Figure 4.2: Convergence tests for the standard-valued algorithm. (Left) Axon Length with respect to time; (right) Cone Concentration as a function of time.

4.3 Parameter Analysis

In this section various experiments will be reported in which one parameter in the model will be variated, in an attempt to uncover possible variations in the results. For Sections 4.3.1 and 4.3.2, only relevant plots for L and Cc will be presented, as discussing all the plots of the tubulin concentration in the axon would be tedious and in some cases unnecessary. In Section 4.3.3 instead the author deemed worthwile to report one plot of the whole concentration for each type of c_0, as this value influences most deeply the inner concentration of tubulin.

4.3.1 Parameter study 1: $l_{0_{max}} \to 0$

To begin with, experiments have been conducted where the initial length of the axon was modified. As in the code the starting length l_0 is determined from the parameters and mesh ($l_0 \leq c_0(0)\ r_g\ z\ \Delta t$), this was implemented by setting a "maximum allowed" to l_0 and dropping that value to zero. Results are in Figure 4.3. As one can see from the plots, l_0 appears to have

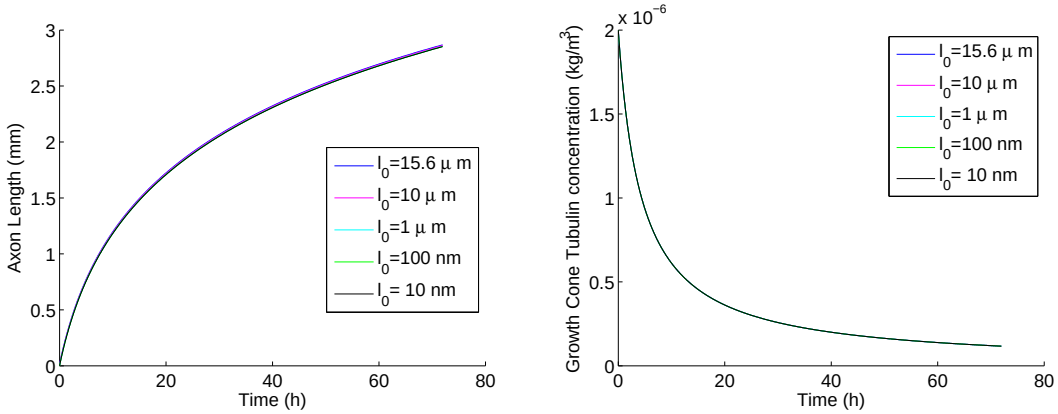

Figure 4.3: Study of the model's reaction to dropping initial axon length. (Left) Axon Length with respect to time; (right) Cone Concentration as a function of time.

next to no effect on the calculation of the axon length itself, but merely as a starting value from where the axon builds up. It could be inferred that while experiments show that $l_0 = 0$ strictly is *not* acceptable, the algorithm exihibits convergence as $l_0 \to 0$.

4.3.2 Paramater study 2: z

In this section, studies conducted on the effects of a decaying growth cone length z will be reported. There will be two distinct plots: in the first (Figure 4.4 results will be shown for values of z not too distant from the standard ones; in Figure 4.5 instead z will be allowed to drop close to 0, up to close-to-unrealistic values. Results indicate that z has a noticeable effect

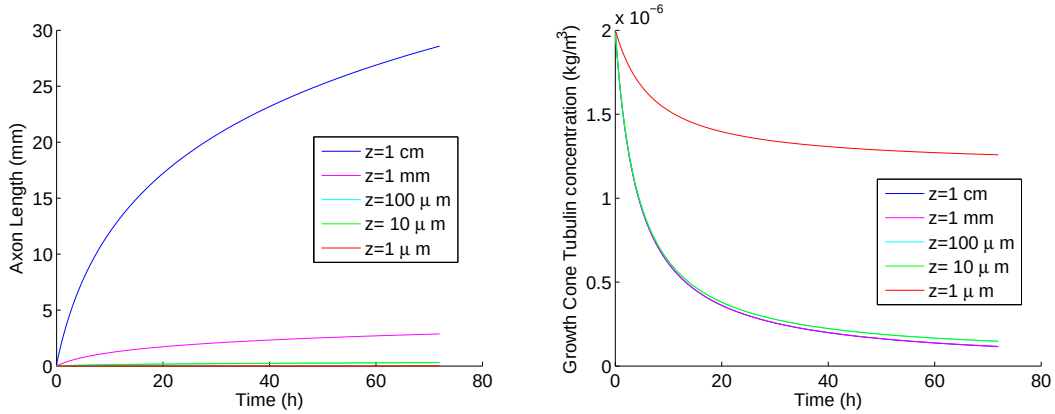

Figure 4.4: Study of the model's reaction to different values of the growth cone's length. (Left) Axon Length with respect to time; (right) Cone Concentration as a function of time.

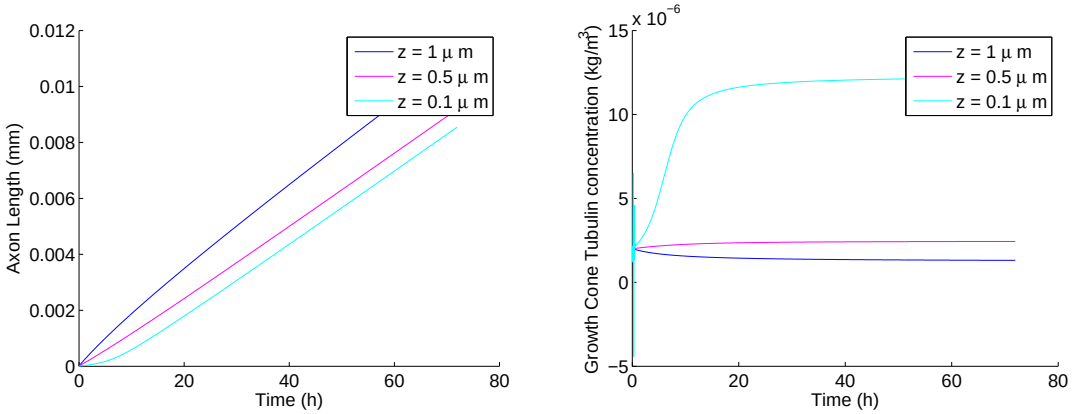

Figure 4.5: Studies with smaller values of z. (Left) Axon Length with respect to time; (right) Cone Concentration as a function of time. Note how the axon length curve changes shape from concave to linear first and convex after, as z becomes smaller. In the right-side plot, the light-blue odd line for the Cone concentration might be caused by numerical errors near $x = 0$.

on how the axon grows: as z becomes smaller, the axon grows progressively slower, but the amount of tubulin in the growth cone seems to increase.

4.3.3 Paramater Study 3: r_g

As mentioned in Table 4.1, the value of the assembly rate for tubulin to microtubules in the growth cone, r_g, has been assumed from other animals' values. However, a keen reader might be wondering what would have happened if different values were used. In this Section these possibilities are discussed. In Figure 4.6 are the plots for different values of this constant. As one can see, r_g has also an effect on how the axon grows, with different orders of magnitude producing different overall axon lengths.

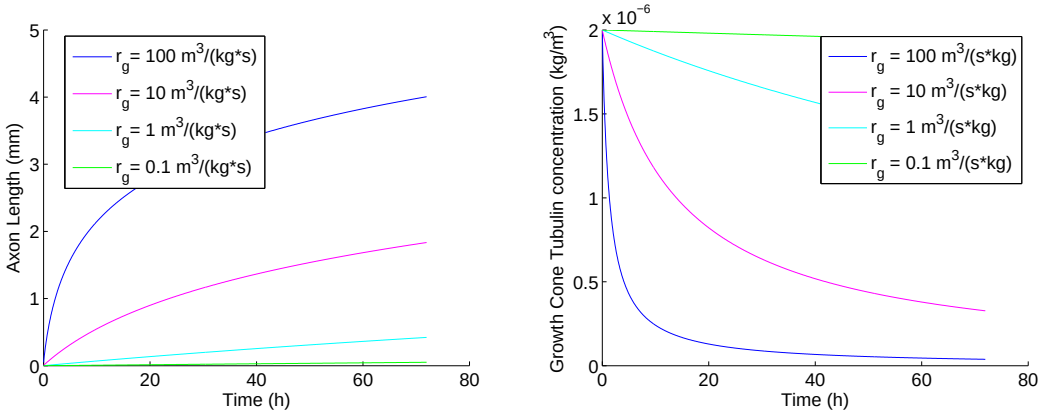

Figure 4.6: Plots describing the effects of different values of r_g. (Left) Axon Length with respect to time; (right) Cone Concentration as a function of time.

4.3.4 Parameter study 4: $c_0(t)$

In this last section, the effect of applying a time-dependent c_0 shall be discussed. In the plots, four different tipes of incoming tubulin have been used:

1. ***Constant.*** Tubulin is injected in the axon by the soma at constant rates:

   (a)
   $$c_0(t) \equiv 2 \cdot 10^{-6} \ \frac{\text{kg}}{\text{m}^3} \ \forall t;$$

   (b)
   $$c_0 \equiv 1 \cdot 10^{-6} \ \frac{\text{kg}}{\text{m}^3};$$

   (c)
   $$c_0 \equiv 0.5 \cdot 10^{-6} \ \frac{\text{kg}}{\text{m}^3};$$

2. ***Linear Decay.*** Let $T \stackrel{def}{=} 1$ day. In this case, tubulin flows in a constant manner during the first day of growth, then the income drops to zero in a linear day over the course of the next day. The c_0 function is:
   $$c_0(t) = \begin{cases} 2 \cdot 10^{-6} & 0 \leq t \leq T \\ 4 \cdot 10^{-6} - \frac{2 \cdot 10^{-6}}{T} t & T \leq t \leq 2T \\ 0 & t \geq 2T \end{cases}$$

3. ***Exponential Decay.*** Tubulin income is $2 \cdot 10^{-6} \ \frac{\text{kg}}{\text{m}^3}$ at the start but decays exponentially with time:
   $$c_0(t) = 2 \cdot 10^{-6} \cdot e^{\left(-\frac{t}{T}\right)};$$

4. ***Sinusoidal Income.*** Tubulin income oscillates between 0 and a certain upper bound over the period of 1 day:

   (a)
   $$c_0(t) = 1 \cdot 10^{-6} + 10^{-6} \cos\left(\frac{2\pi}{T} t\right);$$

(b)

$$c_0(t) = 1 \cdot 10^{-6} + 0.49 \cdot 10^{-6} \cos\left(\frac{2\pi}{T}t\right);$$

In Figure 4.7 are reported the studies for the axon length and cone concentration, as usual. In Figure 4.8 one can find the seven different tubulin concentration plots inside the axon. Note in particular how axon length axis of the tubulin plots in cases 1b, 1c and 4b are shorter than in the other plots, and more so the less tubulin one injects during the first hours of growth (for instance confront 1b and 4b in the first 5 hours). It appears from the results that the first hours of growth are the most critical: if the amount of c_0 is sufficiently high during this period (cases 1a, 2, 3, 4a) then subsequent drops in tubulin income do not affect the growth in a noticeable way (confront for instance 1a and 3); however, if the income at the beginning of the process is lower than this "critical quantity" the growth of the axons becomes progressively slower.

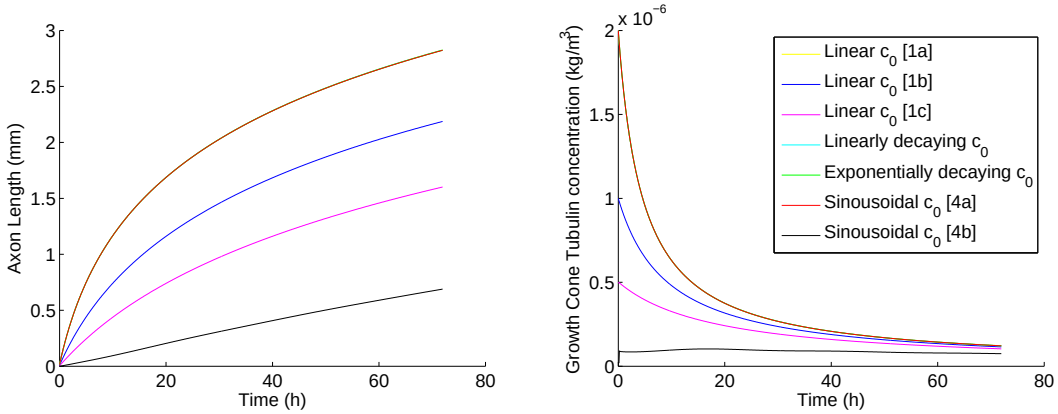

Figure 4.7: Study of the model's reactions to various types of incoming c_0. (Left) Axon Length with respect to time; (right) Cone Concentration as a function of time. Legend has been reported only on the right plot for legibility. Note how the lines corresponding to similarly high levels of incoming tubulin in the first hours of growth (yellow, cyan, green and red) are almost overlapping

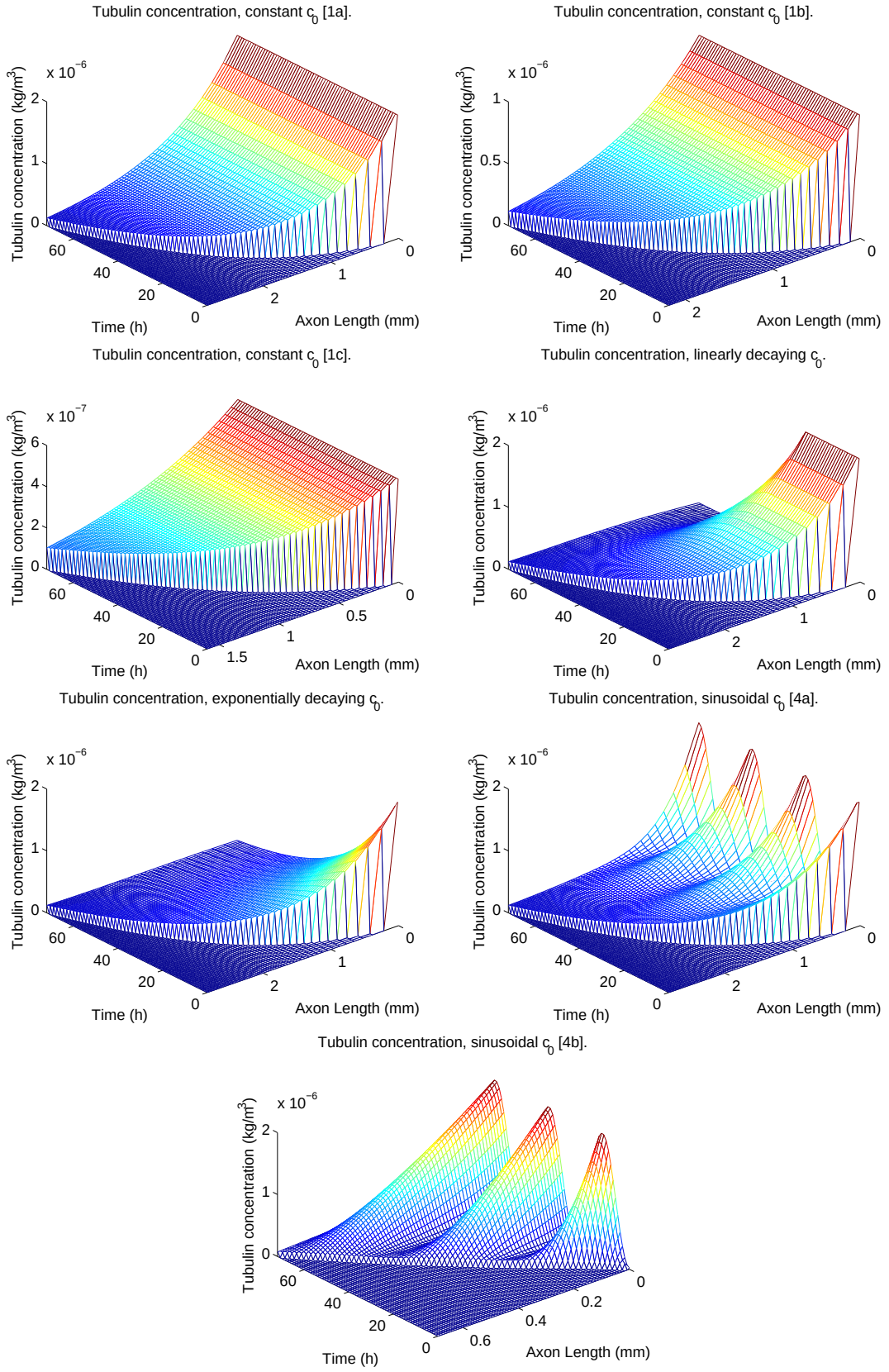

Figure 4.8: Tubulin concentration plots for various types of incoming c_0.

4.4 Conclusions

The plots in this section allow one to conclude a number of things regarding axonal growth, based on the results of the model:

1. The proposed numerical method appears to converge well for standard paramater values; convergence with other values can be also speculated with a comfortable degree of confidence;

2. The starting length l_0 of the axon does not seem to affect the growth, but merely the final length of the axon itself. With this code, the condition is that l_0 must be strictly positive, but the possibility of obtaining results for every value of l_0 suggests that this condition can be removed by adapting the code (perhaps by defining λ_1 differently);

3. The growth cone length z and microtubule assembly rate r_g have a more critical impact on the behaviour of the model itself. Specifically r_g affects the model in the largest way;

4. The incoming soma concentration c_0 seems to be critical only during the early stages of growth. It appears that the less tubulin is provided during the initial hours, the less the overall length of the axon will be. Conversely, a drop in tubulin income which happens further away from the starting time will have little influence on the growth itself, no matter how big or steep the drop itself should be.

4.5 Further Developments

Several open problems remain for subsequent studies on the axonal growth problem. The most important include:

- Understanding wheter or not $l_0 = 0$ can be added as a possible case in the code, possibly by re-defining the λ coefficient so that they can tolerate a null starting length;
- Fitting correct parameter values for the assumed paramater z and r_g, in order to have a more reliable standard set of parameter to begin with;
- Investigate the impact of hidden paramaters of the model, for instance the area A of the axon;
- Calculating the total amount of tubulin mass that has to be provided to the system in order to achieve next to optimal growth or, equivalently, the time window in which the tubulin income level is critical to the growth;
- Investigating the amount of time necessary for the system to stabilize after tubulin stops flowing in from the soma (which happens if the axon has reached its synaptic target);

The model has left open various routes for possible future developments, some of which have been already began but have not been completed for lack of time or resources. Here are some of the most interesting alternatives:

- Further develop the modelling part, for example figuring out which of the $c_0(t)$ is the most akin to the actual tubulin injection, reducing the amount of physical assumptions made or implementing the "dynamical instability" axon phenomenon;
- Having discovered such critical dependance on the growth cone's paramater, improve the growth cone modelling in Sections **2.2.2** and **2.2.3**, for example by considering the growth cone as an actual cable-like structure as opposed to a completely mixed compartment;
- Implement another numerical algorithm and confront results with the one used in this book. Some work has been undertaken in the implementation of an Explicit Euler method which uses the coordinate change
$$\begin{cases} y = \dfrac{x}{l(t)} \\ t' = t \end{cases}$$
to transform the model into a easier, domain-fixed problem. Being completely explicit, this method relies on the *Courant-Frierichs-Levy Condition* to ensure stability for suitable choices of Δy (now uniform in time). Developing and confronting with the earlier method can provide useful informations on the accuracy of both, as well as help with the parameter fitting;
- Implement a higher-dimensional (two or three dimensions in space) model and numerical algorithm. This further development could also provide a link to the field of axon guidance research, a very open and interesting topic for both biological and mathematical research.

Appendices

Appendix A

Matlab Code

In this Appendix the Matlab^{TM}code that has been used for implementing the numerical scheme is reported.

Listing A.1: Matlab Script for solving the Axon Growth model using the Implicit / Explicit Algorithm (see Section 3.3)

```
% Main Script for the simulation of PDE Axonal Growth Model.
% Continuous Non-dimensionalized Model:
% C' + alpha C_x -Fom C_xx = -NC
% Cc' = alphaz Cc -Fomz C_x (x=l) -Rlz l' Cc
% l' = r_g* / Rlz Cc
% C(0,t) = 1
% C(l(t),t) = Cc(t)
%
% Semi-implicit Euler method.
% Author: Stefano Perna (881208p159)

%%% Initializing Parameters. %%%
% Scale factors
linf = 2e-1; % Typical length of the full grown axon; [m]

c0scale = 2*10^(-6); % Tubulin concentration in the soma. [kg/m^3]
                     % This is only a conversion factor, as c0(t)
                     % is defined in a different sub-routine.
tinf = 10000;      % Typical growth time for giant squid axon. [s]

% Physical constants.
D = 8.6E-12;      % Diffusion coefficient (squid). [m^2/s]
Pe = 0.86;        % Péclet number for tubulin the axon. [1]
a = Pe*D/linf;    % Active transport seed. [m/s]
                  % Pe = a*L/D => a = Pe*D/L
g = 1/(33*3600); % Tubulin degradation rate. [1/s]

% Dimensionless parameters.
z = 1E-3/linf;          % Length of the growth cone. [1]
T = 259200/tinf;        % Time of observations. (3 days) [1]
rg = 30*c0scale*tinf;   % Nondimensionalized growth cone
                        % coefficient: rg^* = rg*t0*c0. [1]
alpha = a*tinf/linf;    % Ratio between distance covered by tubulin
                        % via A.T. and typical length. [1]
Fom = D*tinf/(linf^2); % Mass Fourier Number for tubulin
                        % in the axon. [1]
dt=0.025;               % Time step. [1]
l0=c0(0)*rg*z*dt;       % Starting length of the neurite; [1]
```

```
%%% Creating Time Mesh. %%%

N = floor(T/dt); % Number of time steps. [1]
t = dt*(0:N);    % Mesh vector.

%%% Initializing Variables. %%%

C = zeros(N+1,1); % Concentration of tubulin. [1] 1st index = space
                  %                                2nd index = time
C(1,1) = c0(0,f); % C(:,1) = starting value (n=0)

Cc = zeros(N+1,1); % Concentration of tubulin in the growth
                   % cone. [1]
Cc(1) = C(1,1);
dx = l0; % Vector containing the lengths of the spatial mesh.
         % dx(1) ---> dx0 = l0. [1]
L = zeros(N+1,1); % Length of the axon at time
                  % tn = n*dt. [1]
L(1) = l0;        % L(1) = starting value (n=0).

lambda = zeros(N,1); % Vector containing the lambda
                     % coefficients along the mesh.

%%% Starting Algorithm. %%%
% n=1, special case. t0 --> t1 = dt
% Some assignments are different from the general case.

% Calculating new axon length.
L(2) = L(1) + rg*dt*z(f)*Cc(1);
% Calculating new spatial step.
dx(2,1) = L(2) - L(1);
% Initializing lambda coefficients.
lambda(1) = NaN; % Placeholder.
lambda(2) = 2*dt/(dx(2)+dx(1));

% Expanding concentration matrix.
C = [C, zeros(N+1,1)];
% Calculating new growth cone concencentration.
Cc(2)=(1+dt*alpha/z(f)-dt*rg*Cc(1))*Cc(1);
% Imposing Border Conditions.
C(1,2)=c0(t(1),f); C(2,2) = Cc(2);

% Starting time loop.
for n=2:N
    % Calculating new axon length.
    L(n+1)=L(n)+rg*dt*z(f)*Cc(n);

    % Calculating new spatial step.
    dx(n+1)=L(n+1)-L(n);

    % Expanding concentration matrix.
    C = [C, zeros(N+1,1)];

    % Calculating new lambda coefficient.
    lambda(n+1) = 2*dt/(dx(n+1)+dx(n));

    % Calculating new growth cone concencentration.
```

```
    Cc(n+1) = (1+alpha*dt/z(f)-rg*dt*Cc(n))*Cc(n)-...
        lambda(n)*Fom*(C(n,n)-C(n-1,n));

% Imposing Border Conditions.
C(1,n+1)=c0(t(n),f); C(n+1,n+1)=Cc(n+1);

% Generating A^j coefficients (in vectors)
MDiag=zeros(n-1,1);
PlusDiag=zeros(n-2,1);
MinusDiag=zeros(n-2,1);

% Loop over the cells of the system - last one is not
% calculated due to boundary conditions.
for j =1:n-1
    % Main Diagonal - A_0
    MDiag(j)=1+alpha*lambda(j+1)+Fom/dx(j)*...
        (lambda(j+2)+lambda(j+1))+g*tinf*dt;
    % Lower Diagonal - A_-1
    if j~=1
        MinusDiag(j) = -alpha*lambda(j+1)-...
            (Fom*lambda(j+1))/dx(j);
    end
    % Upper Diagonal - A_+1
    if j~=n-1
        PlusDiag(j) = -(Fom*lambda(j+2))/dx(j);
    end
end

% Adjusting Lower Diagonal - must avoid first element = 0
MinusDiag = MinusDiag(2:end);

% Building Gaussian Matrix.
A = diag(MDiag,0)+diag(PlusDiag,+1)+diag(MinusDiag,-1);
% Building border conditions vector.
BCV = zeros(n-1,1);
% n==2 (first loop) is a special case: BCV is a scalar.
if n==2
    BCV= (-alpha*lambda(2)-(Fom*lambda(2+1))/dx(1))*...
        c0(t(2),f)+(-(Fom*lambda(3))/dx(1))*1;
else
    BCV(1) = (-alpha*lambda(2)-(Fom*lambda(2))/dx(1))*...
        c0(t(n),f);
    BCV(end) = -(Fom*lambda(n+1))/dx(n-1)*Cc(n+1);
end

% Solving system.
C(2:n,n+1)=A\(C(2:n,n)-BCV);
end
```

Appendix B

Acknowledgements

B.1 English

This thesis work has been conceived, produced and completed in Sweden, and there I could find many people I wish to personally thank. Some of them have actively helped with the writing of this booklet, some of them have offered me support that I'll never be able to repay, in love or friendship, and some of them instead have been just a pleasant if short company on the long way to these lines. Nevertheless, I think they deserve mentioning.

I would like to thank dearly my supervisor, professor Stefan Diehl at the Centre of Mathematical Sciences (LTH). Since the first time I have written to him, back in August 2012, he has shown availability and attention way beyond his duties, and the work we did together was very representative of a different kind of sensibility and way of thought which I think every modern mathematician should have, at some point. So my many thanks to him, with the hope to continue working together eventually on this or other interesting mathematical problems. Best of luck with your personal research and family life!

Then I want to mention what I consider to be Sweden's best and most important present to me: my dear little Josefin. She has been the light in the shadows on the winter night, the flames of hope when the weather turns too cold and the chill of reason when enthusiasm wants to burn everything. While she hasn't actively participated to the writing of this math paper, her constant support and thoughtfulness have been more then a necessity to get to the end. So I would like to thank her from the deep of my heart, and send her my best wishes that hers - our plans go exactly as we wish, or why not, even better. You deserve nothing less. Jag älskar min lilla söta solros!

I'd like to send special thanks to Josse's family also namely Ulf, Christina and Johan. I'm grateful to them for their kind support and their hospitality, not to mention their readiness to accept me in their beautiful family. I'm sure this means a lot for both of us, but it does in particular for me. Så tack så mycket, jag hoppas att vi kan fortsätta så här under en lång, lång tid.

It would be impossible to continue this acknowledgments without mentioning the people from Vikingavgen's Holy Church, where I spent most of my time in Sweden. It would take an entire report just to tell the stories we have gone throught together, so I'll be content with mentioning everyone of you: Maxie, Jil, Svenja, Franzi, Alex, Thomas & Thomas, Adela, Eugen. One big hug to everyone of you, and may I wish you the best for everything you will be doing in your life. I hope we will meet again one day, at the Church.

One word of thank must go to the new members of the Church, who entered our big family in January. I'm talking of Chris, Farah, Emgee, Adrien and Lisa. I deliver our house to you all, in the hopes you'll keep the fame and honour of the Church as high as it was last semester. Keep rollin', folks.

And one big thanks has to go to all the wonderfull people I met here in Sweden, and with

whom my experience only got better and better. So I'd like to send one big hug to Lauma, Jakub, Gavin, Susanne, Wilhelm, Alice, Karin, Daniél, Daniél, Simon, Thomas, Mia, all the friends from the Multilanguage Café and the Game Nights, the poeple from the Swedish Courses and all the others I'm surely forgetting due to my old age. Thank you everyone, and best of luck with your stay in Lund. I hope we will meet again and raise a toast together to this beautiful country.

One mention goes to my friends from the *Star Wars: The Old Republic* online guild, which I will mention by their online name: M'al (a.k.a. Jordan), Bulgi, Satanio, Delai, Nocturno, Tim, Erik, Habbib, and all the others. Thanks guys, the time we spent together was in no sense less important or worthwhile than with any other real-life friend.

Finally, I'd like to thank Sweden for being the host for this whole periods, for its beautiful landscapes and fine women (one in particular ;)), for its nice and hospitable people and for everything it offers to whoever visits it. It was worth every split of time and effort to be here, and I hope I can stay for much, much longer.

B.2 Italiano

Dopo diciotto anni di studi, un lungo percorso sta per volgere al termine. Ci sarebbe molto di cui parlare, su quello che è successo e sul futuro che si staglia all'orizzonte, ma questa non è la sede.

Quando iniziai i miei studi universitari, cinque anni e mezzo fa, non avevo ben chiaro cosa avrei fatto. Certo, avevo scelto in base alle mie inclinazioni e non seguendo facile promesse di denaro, lavoro o semplicità. Ma nondimeno ero un giovane diplomato con tante idee in testa e niente di concreto in mano. Ora, ad un passo di una laurea Magistrale e con (seppur labili) prospettive di Dottorato, posso dire di non essere più quella persona. Almeno non del tutto.

È quindi mio dovere ma soprattutto mio grande piacere sciovinare i dovuti ringraziamenti. Innanzitutto, i miei più sinceri ringraziamenti vanno ai miei genitori, Pietro ed Anna. Come già dissi in passato, senza il loro supporto ed il loro controllo questo lavoro, tutta la mia carrirera universitaria non sarebbe mai esistita. È semplice limitarsi ad apprezzare vitto, alloggio, pagamento di tasse e quant'altro, ma io credo che il succo sia altrove. A volte capita che le cose vadano male, che la bussola venga smarrita o che la strada sembri troppo dura: in quei momenti anche il peggiore egoista trova sempre un supporto nella sua famiglia, nei suoi genitori. E di questo forse me ne rendo bene conto solo ora. Per questo vi ringrazio dal profondo del cuore, mamma e papà. I matematici non sono molto bravi con le parole, quindi sto sul semplice: vi voglio bene.

Per secondi desidero ringraziare con un veloce ma credo significativa carrellata tutta quella compagine sgangherata che io amo chiamare i miei amici. Vengono da ogni luogo e vanno su mille vie diverse, ma per un motivo o per l'altro sono parte della mia vita e ritengo che parte di tutto questo sia dovuto anche a loro. Un frase per ognuno, sperando che per voi conti quanto conta per me scriverle.

- Mattia, compagno di tante squattrinate avventure negli ultimi sei e più anni: fai fruttare il potenziale che sai di avere, il mondo ha bisogno di più artisti che vedano "al di là del muro";
- Andrea, vecchia roccia e amico di una vita: avanti dritto per la tua strada, con qualche libro in più per capire meglio i tuoi bivi;
- Francesca, Fabio e Michele, delle domeniche davanti alla Play e delle pizzate: grazie per le risate. A volte sono l'unica cosa di cui avevo bisogno;
- Alessandro, mentore, supporto e bastian contrario: non hai bisogno che ti dica nulla, ma sappi che prima o poi diventerò più bravo del mio maestro!

- Paolino, faro guida e supremo maestro Zen del nostro gruppo: la donna della tua vita sarà una campionessa di Magic, ne sono sicuro. Va' fuori e cercala;
- Emanuele, Silvia e Tommaso, il resto del gruppo dei Vanillas: non cambiate mai ragazzi. Fatelo per me;
- Bianca, con il suo pancione: dopo questo basta, ok? Pensa anche un po' a te stessa;
- Enrico con Mara, Alice, Marco con Ste, Francesco con Giulia, Francesca, Sara, Chiara con Luca, Enrica e tutti gli altri della compagnia: al di là di tutte le differenze, siete un bellissimo gruppo e sono onorato che mi abbiate accolto. Un grande abbraccio a tutti;
- Angelo, Mattia, Federico e tutti i compagni della Statale: non vi conosco da una vita come vi conoscete tra voi, ma è stato un piacere studiare con voi. Diventate grandi matematici ed insegnate al mondo a pensare;
- Elisabetta, la piccola biondina di casa: credi di più in te stessa e fidati di più del mondo. C'è davvero qualcuno che ti vuole bene, qua fuori;
- Silvia, che proprio non riesco a capire: non fa niente. Le cose andranno meglio in futuro. Basta solo cominciare a crederci.

Anche la famiglia merita il suo posto nella lista, quindi saluto con affetto Ermes, Elisabetta, Daniele e Holta con Sofia, Maurizio e Michela con la piccola Alice, Maria, Antonio, Rosina, Ilaria con Sole, Rossana, i nonni Peppino e Anna, il piccolo Franco e tutto il resto dei Perna e dei Mazzoleni. Non importa dove andremo, dove andrò a finire, occuperete per sempre un posticino nella memoria e nel cuore.

Un saluto anche a tutti i miei allievi, tra cui cito senza nessuna pretesa di completezza Bianca, Veronica, Valentina, Luca, Louis, Pietro, Andrea e tutti gli altri che mi sono sicuramente scordato. Ognuno di voi può farcela in qualsiasi cosa vogliate fare nella vita, e le nostre lezioni ve l'hanno dimostrato. Continuate così.

Un saluto anche al Coro Giovani di Azzano San Paolo, con il rinnovato augurio di investire sempre di più in voi stessi: è quello il più grande valore che abbiamo e nessuno bigottismo dovrà mai portarcelo via.

Siamo dunque in conclusione in questo scritto. Tante cose sono state dette, tanto lavoro è stato fatto, tante risorse investite. Che dire dunque? Di cosa si parla prima della fine dello spettacolo, quando le tende stanno per chiudersi? In genere si guarda indietro e si comincia a pensare, riassumere, forse commentare. Ma chi mi conosce sa che non è da me rimuginare sul passato. Il futuro è dove andiamo, ed è lì che dobbiamo fissare lo sguardo. In conclusione allora desidero citare un'ultima persona che merita di essere ringraziata. Una persona che ha moltissimi difetti, che non ha mai sviluppato il suo potenziale, che si potrebbe dire lo abbia sprecato. Una persona che non fa scena, che spesso si nasconde dietro le quinte. Una persona un po' strana e forse anche bizzarra, di quelle che non sai se le vuoi avere intorno o se non ti vanno a genio. Eppure questa persona ha avuto il coraggio di andare avanti per la sua strada. Non ha mai accettato di scendere a compromessi con i suoi ideali, anche a costo di sbagliare. Ha spinto dove tutti dicevano "tira". Ha dormito quando tutti dicevano, "svegliati". C'ha creduto quando tutti dicevano, "non funzionerà mai". Ed alla fine questo piccolo, stolto pazzo sognatore, con troppe idee e troppo poca voglia, ha prodotto questo libello. Bello o brutto, utile o meno, l'ha fatto lui, e comunque vada a finire, ne è valsa la pena.

Ne è valsa la pena, Stefano.

Bibliography

[Aes00] M. Aeschlimann. Biophysical Models of Axonal Pathfinding. PhD thesis, Université de Lausanne, 2000.

[ALH52a] A. F. Huxley A. L. Hodgkin. A quantitative description of membrane current and its application to conduction and excitation in nerve. J. Physiol., 117:500–554, 1952.

[ALH52b] B. Katz A. L. Hodgkin, A. F. Huxley. Measuremant of the current-voltage relation in the membrane of the giant axon in *Loligo*. J. Physiol., 116:424–448, 1952.

[BPG06] Arjen van Ooyen Bruce P. Graham. Mathematical modelling and numerical simulation of the morphological development of neurons. BMC Neuroscience, 7:S9, 2006.

[Caj90] S.R. Cajal. À quelle époque apparaissent les expansions des cellules nerveuses de la moelle épinière du poulet? Anatomischer Anzeiger, 21–22:609–639, 1890.

[DRM04] Bruce P. Graham Douglass R. Mclean. Mathematical formulation and analysis of a continuum model for tubulin-driven neurite elongation. Proceedings of the Royal Society A: Mathematical, Physical and Engineering Sciences, 460(2048):2437–2456, 2004.

[HGEH96] A. Fine H. G. E. Hentschel. Diffusion-regulated control of cellular dendritic morphogenesis. Proc. R. Soc. Lond. B 22, 263(1366):1–8, 1996.

[JAG99] et al. James A. Galbraith, Thomas S. Reese. Slow transport of unpolymerized tubulin and polymerized neurofilament in the giant squid axon. Proceedings of the National Academy of Science USA, 96:11589–11594, 1999.

[LVDW80] J. B. Olmsted Livingston Van Der Water. The quantitation of tubulin in neuroblastoma cells by radioimmunossay. The Journal of Biological Chemistry, 255(20):10744–10751, 1980.

[MB07] M.A. Paradiso M.F. Bear, B.W. Connors. Neuroscience Exploring the Brain. Lippincott Williams & Wilkins, 2007.

[MC02] Lanette Fee Michael Caplow. Dissociation of the tubulin dimer is extremely slow, thermodinamically very unfavourable and reversible in the absence of an energy source. Molecular Biology of the Cell, 13:2120–2131, 2002.

[NSS07] *et alii* N. Sánchez-Soriano, G. Tear. Drosophila as a genetic and cellular model for studies on axonal growth. Neural Develop., 2:9, 2007.

[SM04] T. Shinbrot S.M. Maskey, H. M. Buettner. Growth cone pathfinding: a competition between deterministic and stochastic events. BMC Neuroscience, 5:22, 2004.

[Wika] Wikipedia. Axon — Wikipedia, the free encyclopedia.

[Wikb] Wikipedia. Neuron — Wikipedia, the free encyclopedia.

[Wikc] Wikipedia. Squid — Wikipedia, the free encyclopedia.

[Wikd] Wikipedia. Squid — Wikipedia, the free encyclopedia.

[Wike] Wikipedia. Squid — Wikipedia, the free encyclopedia.